

---

# Boosting Randomized Smoothing with Variance Reduced Classifiers

---

Miklós Z. Horváth, Mark Niklas Müller, Marc Fischer, Martin Vechev

Department of Computer Science

ETH Zurich, Switzerland

mihorvat@ethz.ch, {mark.mueller, marc.fischer, martin.vechev}@inf.ethz.ch

## Abstract

Randomized Smoothing (RS) is a promising method for obtaining robustness certificates by evaluating a base model under noise. In this work we: (i) theoretically motivate why ensembles are a particularly suitable choice as base models for RS, and (ii) empirically confirm this choice, obtaining state of the art results in multiple settings. The key insight of our work is that the reduced variance of ensembles over the perturbations introduced in RS leads to significantly more consistent classifications for a given input, in turn leading to substantially increased certifiable radii for difficult samples. We also introduce key optimizations which enable an up to 50-fold decrease in sample complexity of RS, thus drastically reducing its computational overhead. Experimentally, we show that ensembles of only 3 to 10 classifiers consistently improve on the strongest single model with respect to their average certified radius (ACR) by 5% to 21% on both CIFAR-10 and ImageNet. On the latter, we achieve a state-of-the-art ACR of 1.11. We release all code and models required to reproduce our results upon publication.

## 1 Introduction

Modern deep neural networks are successfully applied to an ever-increasing range of applications, but while they often achieve excellent accuracy on the data distribution they were trained on, they have been shown to be very sensitive to slightly perturbed inputs, called adversarial examples [1, 2]. This limits their applicability to safety-critical domains. Heuristic defenses against this vulnerability have been shown to be breakable [3, 4] highlighting the need for provable robustness guarantees.

A promising method providing such guarantees for large networks is randomized smoothing (RS) [5]. The core idea is to provide probabilistic robustness guarantees with arbitrarily high confidence by adding noise to the input of a base classifier and computing the expected classification over the perturbed inputs using Monte Carlo sampling. The key to obtaining high robust accuracies is a base classifier with low variance with respect to these perturbations that remains consistently accurate even under high levels of noise. Existing works use different regularization and loss terms to encourage such behavior [6–8], but are ultimately all limited by the bias-variance trade-off of individual models. We show first theoretically and then empirically how ensembles can be constructed to significantly reduce this variance component and thereby increase certified radii for individual samples and consequently certified accuracy across the whole dataset.

Ensembles are a well-known tool for reducing classifier variance at the cost of increased computational cost [9]. However, in the face of modern architectures [10, 11] allowing the stable training of large models, they have been considered computationally inefficient. Yet, recent work [12] shows ensembles to be more efficient than single monolithic networks in many regimes. In light of this, we develop a theoretical framework analyzing this variance reducing property of ensembles under the perturbations introduced by RS. Further, we show how this reduced variance can significantly

increase the prediction probability of the majority class leading to much larger certified radii than evaluating more perturbations with an individual model.

Certification with RS is computationally costly as the base classifier has to be evaluated many thousand times. To avoid exacerbating these costs by using ensembles as base models, we develop two techniques: (i) an adaptive sampling scheme for RS, which certifies samples for predetermined certification radii in stages reducing the mean certification time up to 50-fold and (ii) a special aggregation mechanism for ensembles which only evaluates the full ensemble on challenging samples, for which there is no consensus between a predefined subset of the constituting models.

**Main Contributions** Our key contributions are:

- A novel, theoretically motivated and statistically sound soft-ensemble scheme for randomized smoothing, reducing perturbation variance and increasing certified radii (§4 and §5).
- A data-dependent adaptive sampling scheme for RS that reduces the sample complexity for predetermined certification radii in a statistically sound manner (§6).
- An extensive evaluation, examining the effects and interactions of ensemble size, training method, and perturbation size. We obtain state-of-the-art results on ImageNet and CIFAR10 for a wide range of settings, including denoised smoothing (§7).

## 2 Related Work

**Adversarial Robustness** Following the discovery of adversarial examples [1, 2], defenses aiming to robustify networks were proposed [13, 14]. Particularly relevant to this work are approaches that certify or enforce robustness properties. We consider probabilistic and deterministic approaches.

Deterministic certification methods compute the reachable set for given input specifications using convex relaxations [15–23], mixed integer linear programming [24], semidefinite programming [25, 26], or satisfiability modulo theories [27, 28], to reason about properties of the output. To obtain networks amenable to such approaches, specialized training methods have been proposed [22, 29–32].

Probabilistic certification [5, 33, 34] introduces noise to the classification process to obtain probabilistic robustness guarantees, allowing the certification of larger models than deterministic methods. We review Cohen et al. [5], which has been extended in numerous ways [35–44], in §3 and associated training methods [6–8, 45] in App. D.3.

**Ensembles** have been extensively analysed with respect to different aggregation methods [46, 47], diversification [48], and the reduction of generalization errors [49, 50]. Randomized Smoothing and ensembles were first combined in Liu et al. [51] as ensembles of smoothed classifiers. However, the method does not retain strong certificates for individual inputs, thus we consider the work to be in a different setting from ours. We discuss this in App. A. While similar at first glance, Qin et al. [52] randomly sample models to ensemble, evaluating them under noise to obtain an empirical defense against adversarial attacks. They, however, do not provide robustness guarantees.

## 3 Randomized Smoothing

In this section, we review the relevant background on Randomized Smoothing (RS) as introduced in Cohen et al. [5]. We let  $f: \mathbb{R}^d \mapsto \mathbb{R}^m$  denote a base classifier that takes an  $d$ -dimensional input and produces  $m$  numerical scores (logits), one for each class. Further, we let  $F(\mathbf{x}) := \arg \max_q f_q(\mathbf{x})$  denote a function  $\mathbb{R}^d \mapsto [1, \dots, m]$  that directly outputs the class with the highest score.

For a random variable  $\epsilon \sim \mathcal{N}(0, \sigma_\epsilon^2 \mathbf{I})$  we define a smoothed classifier  $G: \mathbb{R}^d \mapsto [1, \dots, m]$  as

$$G(\mathbf{x}) := \arg \max_c \mathcal{P}_{\epsilon \sim \mathcal{N}(0, \sigma_\epsilon^2 \mathbf{I})}(F(\mathbf{x} + \epsilon) = c). \quad (1)$$

This classifier  $G$  is then robust to adversarial perturbations as follows:

**Theorem 3.1** (From [5]). *Let  $c_A \in [1, \dots, m]$ ,  $\underline{p}_A, \overline{p}_B \in [0, 1]$ . If*

$$\mathcal{P}_\epsilon(F(\mathbf{x} + \epsilon) = c_A) \geq \underline{p}_A \geq \overline{p}_B \geq \max_{c \neq c_A} \mathcal{P}_\epsilon(F(\mathbf{x} + \epsilon) = c),$$

*then  $G(\mathbf{x} + \delta) = c_A$  for all  $\delta$  satisfying  $\|\delta\|_2 \leq R$  with  $R := \frac{\sigma_\epsilon}{2}(\Phi^{-1}(\underline{p}_A) - \Phi^{-1}(\overline{p}_B))$ .*

Here, given  $\mathbf{x}$ , if an attacker selects  $\mathbf{x}'$  from  $\{\mathbf{x} + \eta \mid \|\eta\|_2 \leq \delta\}$ , then showing  $R \geq \delta$  in Theorem 3.1, certifies that  $G(\mathbf{x}) = G(\mathbf{x}')$ .

Computing the exact probabilities  $\mathcal{P}_\epsilon(F(\mathbf{x} + \epsilon) = c)$  is generally intractable. Thus, to allow practical application, CERTIFY [5] (see Algorithm 1) utilizes sampling:  $n_0$  samples to determine the majority class, then  $n$  samples to compute a lower bound  $\underline{p}_A$  with confidence  $1 - \alpha$  via the Clopper-Pearson lemma [53]. If  $\underline{p}_A > 0.5$ , we set  $\overline{p}_B = 1 - \underline{p}_A$  and obtain radius  $R = \sigma_\epsilon \Phi^{-1}(\underline{p}_A)$  via Theorem 3.1 else we abstain (return  $\emptyset$ ).

To obtain high certified radii, the base model  $F$  must be trained to cope with the added Gaussian noise  $\epsilon$ . To achieve this, several training methods [5–8, 45], discussed in App. D.3, have been introduced.

---

**Algorithm 1** Certify from [5]

---

```

1: function CERTIFY( $F, \sigma_\epsilon, \mathbf{x}, n_0, n, \alpha$ )
2:  $\text{cnts0} \leftarrow \text{SAMPLEUNDERNOISE}(F, \mathbf{x}, n_0, \sigma_\epsilon)$ 
3:  $\hat{c}_A \leftarrow \text{top index in cnts0}$ 
4:  $\text{cnts} \leftarrow \text{SAMPLEUNDERNOISE}(F, \mathbf{x}, n, \sigma_\epsilon)$ 
5:  $\underline{p}_A \leftarrow \text{LOWERCONFBNB}(\text{cnts}[\hat{c}_A], n, 1 - \alpha)$ 
6: if  $\underline{p}_A > \frac{1}{2}$  then
7:   return prediction  $\hat{c}_A$  and radius  $\sigma_\epsilon \Phi^{-1}(\underline{p}_A)$ 
8: return  $\emptyset$ 

```

---

## 4 Randomized Smoothing for Ensemble Classifiers

In this section, we extend the methods discussed in §3 from single models to ensembles before delving into the theoretical analysis in §5 and an efficient evaluation strategy in §6.

For a set of  $k$  classifiers  $\{f^l: \mathbb{R}^d \mapsto \mathbb{R}^m\}_{l=1}^k$ , we construct an ensemble  $\bar{f}$  via weighted aggregation,  $\bar{f}(\mathbf{x}) = \sum_{l=1}^k w^l \gamma(f^l(\mathbf{x}))$ , where  $w^l$  are the weights and  $\gamma: \mathbb{R}^m \mapsto \mathbb{R}^m$  is a post-processing function. Soft-voting (where  $\gamma$  denotes identity) and equal weights  $w^l = \frac{1}{k}$  perform experimentally well (see App. E.3.1) while mathematically simple. Thus, we consider averaging of the logits:

$$\bar{f}(\mathbf{x}) = \frac{1}{k} \sum_{l=1}^k f^l(\mathbf{x}) \quad (2)$$

The ensemble  $\bar{f}$ , and its corresponding hard-classifier  $\bar{F}(\mathbf{x}) := \arg \max_q \bar{f}_q(\mathbf{x})$ , can be used without further modification as base classifiers for RS. In the following section, we will show that the ensemble has reduced variance with respect to the perturbations  $\epsilon$ , and thus will predict the majority class  $\hat{c}_A$  more often, increasing both the true majority class probability  $p_A$  and its lower confidence bound  $\underline{p}_A$ , key for increasing the certified radius as per Theorem 3.1.

While not required for the theoretical analysis we assume all  $k$  classifiers to use identical architecture, hyperparameters and training loss function. We find that different random seeds and the training methods introduced in App. D.3 produce sufficiently diverse classifiers of similar performance.

**$K$ -consensus Aggregation** To reduce both inference and certification times, we can adapt the ensemble aggregation process to return an output early when there is consensus. Concretely, we first order the classifiers in an ensemble by their accuracy (under noisy inputs) on a holdout dataset. Then, when evaluating  $\bar{f}$ , we query classifiers in this order. If the first  $K$  individual classifiers agree on the predicted class, we perform soft-voting on these and return the result without evaluating the remaining classifiers. Especially for large ensembles, this approach can significantly reduce inference time without hampering performance, as the ratio  $\frac{k}{K}$  can be large.

We note that (i) similar approaches for only evaluating part of an ensemble have been proposed [47, 54, 55], and (ii) that the approach does not affect the mathematical guarantees of RS.

## 5 Variance Reduction via Ensembles for Randomized Smoothing

We now show why ensembles  $\bar{f}$  (cf. Eq. (2)) are well-suited as base classifiers for RS. To this end, we first model the output of  $\bar{f}$  and an individual  $f^l$  as general distributions characterized by their mean and variance. Then, we assume Gaussian distributions and instantiate them with estimated parameters, illustrating the variance reduction on an ensemble of ResNet20. Doing so allows us to understand and predict the observed performance gains. For this analysis, we ignore  $K$ -consensus aggregation. We defer algebraic derivations between the steps shown in this section to App. B.

Our modeling approach mathematically is closely related to Tumer and Ghosh [50], which focus on analyzing ensemble over the whole dataset. In contrast, we condition on one input to study the interplay between the stochasticity in training and random perturbations encountered in RS.

**Individual Classifier** We consider individual classifiers  $f^l: \mathbb{R}^d \mapsto \mathbb{R}^m$  and perturbed inputs  $\mathbf{x} + \epsilon$  for an arbitrary but fixed  $\mathbf{x}$  with Gaussian perturbations  $\epsilon \sim \mathcal{N}(0, \sigma_\epsilon^2 \mathbf{I})$ . We model the logits  $f^l(\mathbf{x}) =: \mathbf{y}^l \in \mathbb{R}^m$  as the sum of two random variables:  $\mathbf{y}^l = \mathbf{y}_p^l + \mathbf{y}_c^l$  and drop the superscript  $l$  while discussing an individual classifier to avoid clutter. Note that the split in  $\mathbf{y}_c + \mathbf{y}_p$  becomes essential when analysing the ensemble where we differentiate between the correlation structures for the two terms.

The behaviour on a specific clean sample  $\mathbf{x}$  is modeled by  $\mathbf{y}_c$  with mean  $\mathbf{c} \in \mathbb{R}^m$ , the expectation of the logits for this sample over the randomization in the training process, and corresponding covariance  $\Sigma_c$ . The impact of the perturbations  $\epsilon$  introduced during RS is modelled by  $\mathbf{y}_p$  with mean zero and covariance  $\Sigma_p$ . We do not restrict the structure of the covariance matrices and use standard notation:  $(\Sigma_p)_{ii} = \sigma_{p,i}^2$  and  $(\Sigma_p)_{ij} = \sigma_{p,i}\sigma_{p,j}\rho_{p,ij}$  on the example of  $\Sigma_p$ . We note that while  $\sigma_{p,i}$  may depend on  $\sigma_\epsilon$ , both  $\sigma_{c,i}$  and  $\sigma_{p,i}$  are distinct from it. As  $\mathbf{y}_p$  models the local behaviour under small perturbations and  $\mathbf{y}_c$  models the global training effects, we assume them to be independent. We thus obtain logits  $\mathbf{y}$  with mean  $\mathbf{c}$ , the expectation over the training process for the clean sample, and covariance matrix  $\Sigma = \Sigma_c + \Sigma_p$ , where  $\Sigma_c$  and  $\Sigma_p$  encode the stochasticity of the training process and perturbations respectively.

The classifier prediction  $F^l(\mathbf{x}) = \arg \max_q y_q$  is determined by the differences between logits. We call the difference between the target logit and others the classification margin. During certification with RS, the first step is to determine the majority class. Without loss of generality, we will in the following assume, that it has been determined to index 1 leading to the classification margin,  $z_i = y_1 - y_i$ . If  $z_i > 0$  for all  $i \neq 1$ , the majority class logit  $y_1$  is larger than those of all other classes  $y_i$ . Under the above assumptions, the statistics of the classification margin for a single classifier are:

$$\begin{aligned}\mathbb{E}[z_i] &= c_1 - c_i \\ \text{Var}[z_i] &= \sigma_{p,1}^2 + \sigma_{p,i}^2 + \sigma_{c,1}^2 + \sigma_{c,i}^2 - 2\rho_{p,1i}\sigma_{p,1}\sigma_{p,i} - 2\rho_{c,1i}\sigma_{c,1}\sigma_{c,i}\end{aligned}$$

**Ensemble** Now, we construct an ensemble of  $k$  of these classifiers. We use soft-voting (cf. Eq. (2)) to compute the ensemble output  $\bar{\mathbf{y}} = \frac{1}{k} \sum_{l=1}^k \mathbf{y}^l$  and then the corresponding classification margins  $\bar{z}_i = \bar{y}_1 - \bar{y}_i$ . By the linearity of expectation  $\mathbb{E}[\bar{z}_i] = \mathbb{E}[z_i] = c_1 - c_i$ . We assume  $\mathbf{y}_p^i$  and  $\mathbf{y}_p^j$  to be correlated with  $\zeta_p \Sigma_p$  for classifiers  $i \neq j$  and similarly model the correlation of  $\mathbf{y}_c^i$  and  $\mathbf{y}_c^j$  with  $\zeta_c \Sigma_c$  for  $\zeta_p, \zeta_c \in [-1, 1]$ . We thereby obtain the following variance:

$$\text{Var}[\bar{z}_i] = \underbrace{\frac{k + 2\binom{k}{2}\zeta_p}{k^2}(\sigma_{p,1}^2 + \sigma_{p,i}^2 - 2\rho_{p,1i}\sigma_{p,1}\sigma_{p,i})}_{\sigma_p^2(k)} + \underbrace{\frac{k + 2\binom{k}{2}\zeta_c}{k^2}(\sigma_{c,1}^2 + \sigma_{c,i}^2 - 2\rho_{c,1i}\sigma_{c,1}\sigma_{c,i})}_{\sigma_c^2(k)}.$$

**Variance Reduction** We can split  $\text{Var}[\bar{z}_i]$  into the components associated with the perturbation effect  $\sigma_p^2(k)$  and the clean prediction  $\sigma_c^2(k)$ , both as functions of the ensemble size  $k$ . We now compare these variance terms independently to the corresponding terms of an individual classifier dropping the subscripts  $c$  and  $p$  from  $\sigma_p^2(k)/\sigma_p^2(1)$  and  $\sigma_c^2(k)/\sigma_c^2(1)$  as they follow the same structure:

$$\frac{\sigma^2(k)}{\sigma^2(1)} = \frac{(1 + \zeta(k-1))(\sigma_1^2 + \sigma_i^2 - 2\rho_{1i}\sigma_1\sigma_i)}{k(\sigma_1^2 + \sigma_i^2 - 2\rho_{1i}\sigma_1\sigma_i)} = \frac{1 + \zeta(k-1)}{k} \xrightarrow{k \rightarrow \infty} \zeta$$

We observe that both variance components go towards their corresponding correlation coefficients  $\zeta_p$  and  $\zeta_c$  as ensemble size grows, highlighting the importance of diverse classifiers.

Especially for samples that are near a decision boundary, this variance reduction will lead to much more consistent predictions, in turn significantly increasing the lower confidence bound on the success probability and thereby the certified radius as per Theorem 3.1.

**Gaussian Perturbation Error** By assuming all  $\mathbf{y}_p^l$  and  $\mathbf{y}_c^l$  to be multivariate Gaussian, it follows that all random variables derived above are also multivariate Gaussian with the respective mean and (co)variance. Theoretically, this follows from Gaussian perturbations for a locally linear model for  $\mathbf{y}_p^l$

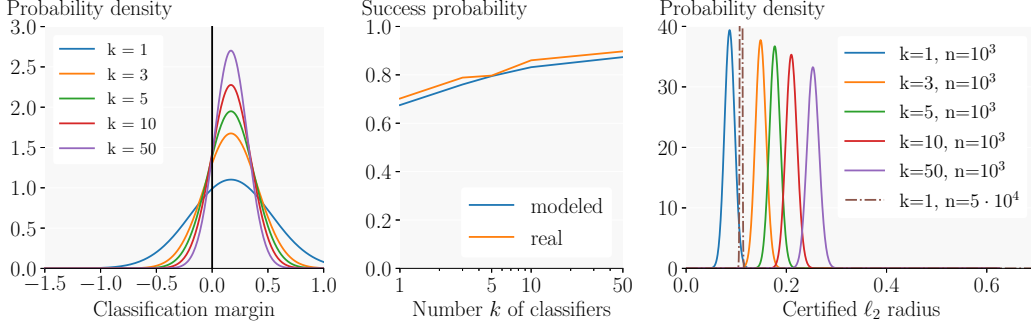


Figure 1: Comparison of the (a) modeled distribution over the classification margin to the runner up class, (b) the resulting success probability of predicting the majority class for a given perturbation, and (c) the corresponding distribution over certified radii for ensembles of different size.

and is an empirically well fitting choice for both. With these assumptions, we obtain the probability of an ensemble of  $k$  classifiers predicting the majority class 1 as:

$$p_1 := \mathcal{P}(\bar{F}(\mathbf{x} + \epsilon) = 1) = \mathcal{P}(\bar{z}_i > 0 : \forall 2 \leq i \leq m) = \int_{\substack{\bar{\mathbf{z}} \text{ s.t. } \bar{z}_i > 0, \\ \forall 2 \leq i \leq m}} \mathcal{P}_{\bar{\mathbf{Z}} \sim \mathcal{N}(\bar{\mu}, \bar{\Sigma})}(\bar{\mathbf{Z}} = \bar{\mathbf{z}}) d\bar{\mathbf{z}}. \quad (3)$$

Knowing this probability,  $p_1$ , of predicting a noisy sample as majority class, we can calculate a probability distribution over the certifiable radii reported by CERTIFY (up to choosing an incorrect majority class  $\hat{c}_A$ ) for a given confidence level  $\alpha$ , sample number  $n$  and perturbation variance  $\sigma_\epsilon^2$  as:

$$\mathcal{P}(R = \sigma_\epsilon \Phi^{-1}(p_1(n_1, n, \alpha))) = \mathcal{B}(n_1, n, p_1), \quad \text{for } R > 0 \quad (4)$$

with the probability  $\mathcal{B}(s, r, p)$  of drawing  $s$  successes in  $r$  trials from a Binomial distribution with success probability  $p$ , and the lower confidence bound  $p(s, r, \alpha)$  to the success probability of a Bernoulli experiment given  $s$  successes in  $r$  trials with confidence  $\alpha$  according to the Clopper-Pearson interval [53]. We now replace the free parameters,  $c, \Sigma_c, \Sigma_p, \zeta_c, \zeta_p$ , in these formulas with estimates from a real ensemble to show the modeling fit.

**Empirical Analysis** To instantiate our theoretical analysis, we consider an ensemble of up to  $k = 50$  GAUSSIAN trained ResNet20 (for details see §7) at  $\sigma_\epsilon = 0.25$ . We estimate  $c$  and  $\Sigma_c$  as the mean and covariance of the output on a randomly chosen sample  $\mathbf{x}$ . Subtracting the clean outputs from those for the perturbed samples and enforcing zero mean, we estimate the covariance matrix  $\Sigma_p$ . We determine  $\zeta_c$  and  $\zeta_p$  by computing all pairwise covariances between all logits of two classifiers and computing the median ratio between the obtained inter-classifier covariance with the intra-classifier covariance. We observe  $\zeta_c \approx 0$  and  $\zeta_p \approx 0.82 (\pm 0.048 \text{ standard error})$ . We note that  $\zeta_c \approx 0$  implies that our models can be treated as independent conditioned on a fixed input.

Plugging these estimates into our model, under the Gaussian assumption, we observe a significant decrease in the variance of the classification margin to the runner up class (see Fig. 1 (a)). The majority class success probability (see Eq. (3)) for an individual perturbation is effectively equal to the area under the corresponding curve on the right hand side of the decision threshold  $\bar{z} = 0$ , and increases significantly as variance decreases with ensemble size (see Fig. 1 (b)). This increase in turn translates into much larger expected certified radii (see Fig. 1 (c)) for a given number of sampled perturbations (here  $n = 10^3$ ) via Eq. (4). In contrast, sampling more perturbations will, in the limit, only recover the true success probability. In our example, going from one classifier to an ensemble of 50 increases the expected certified radius by 191% while increasing the number of perturbations drawn for a single model only yields a 28% increase (see Fig. 1 (c)). These effects are strongest close to the decision boundary ( $p_A \ll 1$ ) where small increases in  $p_A$  impact the certified radius more than the number of samples  $n$ . As illustrated Fig. 2, this reverses if  $p_A \approx 1$  already for an individual classifier.

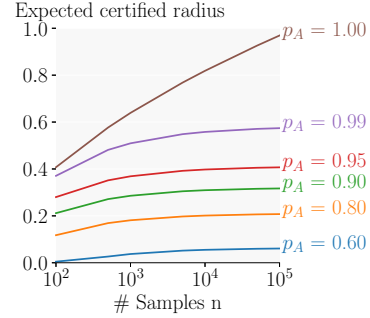


Figure 2: Expected certified radius over the number  $n$  of samples for the true success probabilities  $p_A$ .

---

**Algorithm 2** Adaptive Sampling

---

```

1: function CERTIFYADP( $F, \sigma_\epsilon, \mathbf{x}, n_0, \{n_j\}_j, s, \alpha, \beta, r$ )
2:    $\text{cnts0} \leftarrow \text{SAMPLEUNDERNOISE}(F, \mathbf{x}, n_0, \sigma_\epsilon)$ 
3:    $\hat{c}_A \leftarrow \text{top index in cnts0}$ 
4:   for  $i \leftarrow 1$  to  $s$  do
5:      $\text{cnts} \leftarrow \text{SAMPLEUNDERNOISE}(F, \mathbf{x}, n_i, \sigma_\epsilon)$ 
6:      $\underline{p}_A \leftarrow \text{LOWERCONFBND}(\text{cnts}[\hat{c}_A], n_i, 1 - \frac{\alpha}{s})$ 
7:     If  $\sigma_\epsilon \Phi^{-1}(\underline{p}_A) \geq r$  then return  $\hat{c}_A$ 
8:      $\overline{p}_A \leftarrow \text{UPPERCONFBND}(\text{cnts}[\hat{c}_A], n_i, 1 - \frac{\beta}{s-1})$ 
9:     If  $\sigma_\epsilon \Phi^{-1}(\overline{p}_A) < r$  then return  $\emptyset$ 
10:  return  $\emptyset$ 

```

---

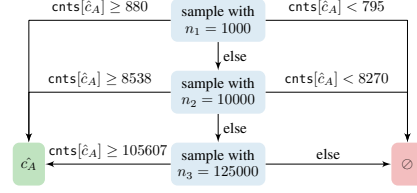


Figure 3: CERTIFYADP with  $\beta = 0.0001$  obtains similar guarantee as CERTIFY at  $n = 100'000$  while being more sample efficient for most inputs. Both use  $\alpha = 0.001, \sigma_\epsilon = r = 0.25$ .

## 6 Adaptive Sampling for Certification Time Reduction

We now propose an adaptive sampling scheme for certification with RS. We assume a target certification radius  $r$  and aim to show  $R \geq r$  via Theorem 3.1. Instead of invoking CERTIFY (see Algorithm 1) with a large  $n$ , we can use CERTIFYADP (see Algorithm 2). After choosing the majority class  $\hat{c}_A$  as in CERTIFY, CERTIFYADP performs an  $s \geq 1$  step procedure: At step  $i$ , we evaluate  $n_i$  fresh samples and, depending on these, either certify radius  $r$ , abort certification, or continue. After  $s$  steps, we abstain. The following theorem summarizes the key properties of the algorithm:

**Theorem 6.1.** For  $\alpha, \beta \in [0, 1], s \in \mathbb{N}^+, n_1 < \dots < n_s$ , CERTIFYADP:

1. returns  $\hat{c}_A$  if at least  $1 - \alpha$  confident that  $G$  is robust with radius at least  $r$ .
2. returns  $\emptyset$  before stage  $s$  only if at least  $1 - \beta$  confident that  $G$  is not robust at radius  $r$ .
3. for  $n_s \geq \lceil n(1 - \log_\alpha(s)) \rceil$  has maximum certifiable radii at least as large as CERTIFY for  $n$ .

We provide a proof in App. C. For well-chosen parameters, this allows certifying radius  $r$  with, in expectation, significantly fewer evaluations of  $F$  than CERTIFY as often  $n_i \ll n$  samples are sufficient to certify or show that certification will not be successful. At the same time, due to (3), the ability to certify large radii (compared to CERTIFY) is not sacrificed. For an example see Fig. 3.

## 7 Experimental Evaluation

We now evaluate the proposed methods on the CIFAR10 [56] and ImageNet [57] datasets considering two key metrics in line with prior work: (i) the certified accuracy at predetermined radii  $r$  and (ii) the average certified radius (ACR). We show, that on both datasets all ensembles outperform their strongest constituting model, obtaining state-of-the-art results. On CIFAR10, we demonstrate, that ensembles of 5 smaller networks (ResNet20) typically outperform one larger network (ResNet110) with fewer total parameters. Further, using adaptive sampling and K-Consensus aggregation speeds up certification up to 50-fold for ensembles and up to 30-fold for individual models.

**Experimental Setup** We evaluate our approach on CIFAR10 with ensembles of ResNet20 and ResNet110 and on ImageNet with ensembles of ResNet50 [10], implemented in PyTorch [58] running on 1 and 2 GeForce RTX 2080 Ti respectively. Due to the significant computational cost of CERTIFY, we follow previous work [5, 6] and evaluate every 20<sup>th</sup> image of the CIFAR10 test set and every 100<sup>th</sup> of the ImageNet test set [5, 8] (500 samples total). We train models with GAUSSIAN [5] as well as CONSISTENCY [8] methods and utilize pretrained MACER [7] and SMOOTHADV [6] models. More details are provided in App. D.4. If not declared differently, we use  $n_0 = 100, n = 100'000, \alpha = 0.001$ , no CERTIFYADP or  $K$ -consensus and evaluate and train with the same  $\sigma_\epsilon$ .

**Results on CIFAR10** We analyze the impact of ensemble size for ResNet20 and ResNet110, trained with GAUSSIAN and CONSISTENCY on CIFAR10, comparing ACR and certified accuracy at  $r = 0.25$  and  $r = 0.75$  in Fig. 4. Across all settings, we initially see significant improvements with increasing ensemble size before observing diminishing returns. For all training methods and architectures, we observe a stronger improvement at large radii, where larger  $\underline{p}_A$  are required for certification, which agrees well with our theoretical observations made in §5. For more detailed results see App. E.3.

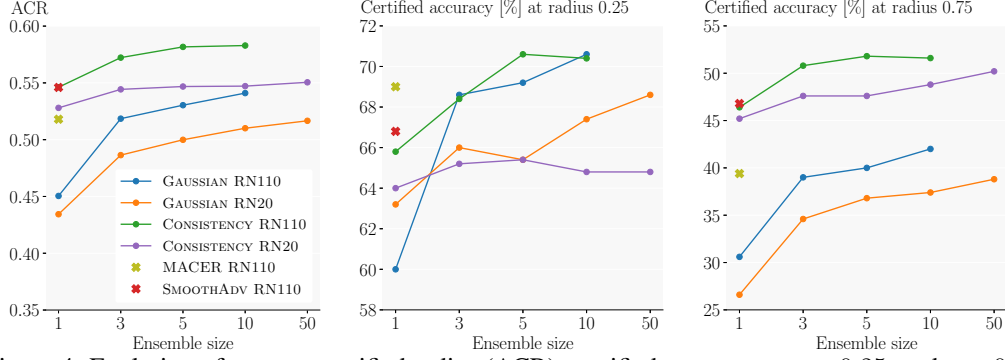


Figure 4: Evolution of average certified radius (ACR), certified accuracy at  $r = 0.25$ , and  $r = 0.75$  with ensemble size  $k$  for various underlying models and  $\sigma_\epsilon = 0.25$  on CIFAR10.

Table 1: CIFAR10 average certified radius (ACR) and certified accuracy at different radii for ensembles of  $k$  models ( $k = 1$  are individual models) at  $\sigma_\epsilon = 0.5$ . Larger is better.

Training	Architecture	$k$	ACR	Radius $r$							
				0.0	0.25	0.50	0.75	1.00	1.25	1.50	1.75
GAUSSIAN	ResNet110	1	0.535	65.8	54.2	42.2	32.4	22.0	14.8	10.8	6.6
		10	<b>0.648</b>	<b>69.0</b>	<b>60.4</b>	<b>49.8</b>	40.0	29.8	19.8	15.0	9.6
	ResNet20	1	0.534	65.2	55.0	43.0	33.0	22.4	16.2	9.6	5.0
		5	0.615	67.6	58.4	47.4	38.8	27.4	19.8	13.2	7.0
CONSISTENCY	ResNet110	50	0.630	67.2	59.4	48.6	39.2	29.0	21.6	14.6	8.2
		10	<b>0.756</b>	65.0	59.0	49.4	<b>44.8</b>	38.6	32.0	26.2	19.8
	ResNet20	1	0.691	62.6	55.2	47.4	41.8	34.6	28.4	21.8	16.8
		5	0.723	62.2	55.0	48.6	42.6	36.4	29.8	23.4	20.6
MACER	ResNet110	50	0.729	61.6	55.8	49.2	43.0	37.8	30.6	24.2	20.0
		1	0.668	62.4	54.4	48.2	40.2	33.2	26.8	19.8	13.0
SMOOTHADV	ResNet110	1	0.725	57.4	50.6	45.8	42.4	37.6	32.2	27.8	22.0
		3	0.742	53.8	49.0	46.2	43.2	<b>39.8</b>	<b>34.4</b>	<b>29.8</b>	<b>25.8</b>

In Table 1, we compare ensembles of 10 ResNet110 and 5 or 50 ResNet20 against individual networks at  $\sigma_\epsilon = 0.5$ , w.r.t. average certified radius (ACR) and certified accuracy at various radii, also visualized in Fig. 5. For additional results on  $\sigma_\epsilon = 0.25$  and  $\sigma_\epsilon = 1.0$  see App. E.1. We consistently observe that ensembles outperform their constituting models or even models with more total parameters. Ensembles of 5 ResNet20 outperform single ResNet110, while the expected diminishing returns in variance reduction lead to 10 ResNet110 outperforming 50 ResNet20. We observe particularly significant improvements on GAUSSIAN trained models, which are not explicitly regularized for consistent predictions, reaching ACR increases of up to 21.1% (ResNet110) and achieve a new state-of-the-art ACR of 0.756 for  $\sigma_\epsilon = 0.5$  using an ensemble of 10 CONSISTENCY trained ResNet110.

**Results on ImageNet** In Table 3 we compare ensembles of 3 ResNet50 with individual models trained using CONSISTENCY, GAUSSIAN, and SMOOTHADV training at  $\sigma_\epsilon = 1.0$ , w.r.t. ACR and certified accuracy, visualizing these results in Fig. 6. We observe similar trends to CIFAR10, with ensembles outperforming their constituting models and the ensemble of 3 CONSISTENCY trained ResNet50 obtaining a new state-of-the-art ACR of 1.11. We present more detailed results in App. E.2.

**$K$ -Consensus Aggregation** In Table 2, we compare certification time reduction and ACR for ensembles of 10 ResNet110 and 50 ResNet20 trained using CONSISTENCY across different  $K$ . KCR denotes the percentage of inputs for which only  $K$  classifiers were evaluated. Even when using only  $K = 2$  we already obtain 81% and 70% of the ACR improvement obtainable by always evaluating the full ensemble ( $k = 10$  and  $k = 50$ ) respectively. The more conservative  $K = 10$  for ResNet20 still reduces certification times by a factor of 2 without losing accuracy. See App. E.4 for more detail.

Table 2:  $K$ -Consensus aggregation at  $\sigma_\epsilon = 0.25$  on CIFAR10.

Architecture	$K$	ACR	Time <sub>RF</sub>	KCR
CONSISTENCY ResNet110	1	0.546	10.0	100.0
	2	0.576	3.25	85.8
	5	0.583	1.59	74.2
	10	0.583	1.00	0.0
CONSISTENCY ResNet20	1	0.528	50.0	100.0
	2	0.544	6.50	87.7
	10	0.551	2.01	69.8
	50	0.551	1.00	0.0

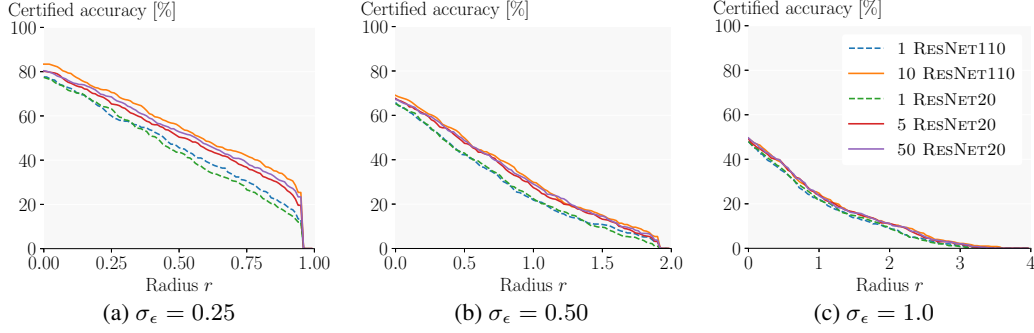


Figure 5: CIFAR10 certified accuracy over certified radius  $r$  for GAUSSIAN trained models.

Table 3: ImageNet average certified radius (ACR) and certified accuracy at different radii for ensembles of  $k$  ResNet50 ( $k = 1$  are individual models) at  $\sigma_\epsilon = 1.0$ . Larger is better.

Training	$k$	ACR	Radius $r$							
			0.0	0.50	1.00	1.50	2.00	2.50	3.00	3.50
GAUSSIAN	1	0.875	43.6	37.8	32.6	26.0	19.4	14.8	12.2	9.0
CONSISTENCY	1	1.022	43.2	39.8	35.0	29.4	24.4	22.2	16.6	13.4
	3	<b>1.108</b>	44.6	40.2	<b>37.2</b>	<b>34.0</b>	<b>28.6</b>	23.2	20.2	16.4
SMOOTHADV	1	1.011	40.6	38.6	33.8	29.8	25.6	20.6	18.0	14.4
	3	1.065	38.6	36.0	34.0	30.0	27.6	<b>24.6</b>	<b>21.2</b>	<b>18.8</b>
MACER <sup>†</sup>	1	1.008	<b>48</b>	<b>43</b>	36	30	25	18	14	-

<sup>†</sup> As reported by Zhai et al. [7].

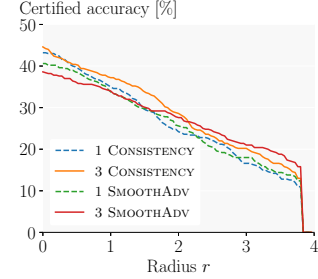


Figure 6: Cert. accuracy over  $r$  for  $\sigma_\epsilon = 1.0$  on ImageNet.

**Adaptive Sampling** We now evaluate the effectiveness of CERTIFYADP first in isolation on individual models and then in conjunction with  $K$ -Consensus aggregation on ensembles using  $\beta = 0.0001$ . In Table 4 we show the effect of applying CERTIFYADP for different sampling count sets, certification radii and training methods to an individual ResNet110 on CIFAR10 at  $\sigma_\epsilon = 0.25$ , providing extended results in App. E.5. We compare  $\text{ASR}_j$ , the portion of samples returned in stage  $j$  and SampleRF and TimeRF, the factor by which sample complexity and certification time are reduced. We generally observe larger speed ups for smaller radii (up to a factor 28 at  $r = 0.25$ ). There, certification only requires small  $p_A$ , which can be obtained even with few samples. For large radii (w.r.t  $\sigma_\epsilon$ ), higher  $p_A$  have to be shown requiring more samples even at true success rates of  $p_A = 1$ , and the first phase only yields early abstentions. This dynamic also explains why the higher success probabilities of CONSISTENCY trained networks lead to larger speed-ups at small radii while at large radii, the lower success probability of GAUSSIAN trained networks allow for more samples to be rejected early. We find  $n_j = \{1'000, 10'000, 125'000\}$  performs well across many different settings.

In Table 5, we consider the combination of CERTIFYADP and  $K$ -Consensus aggregation on ensembles of 10 CONSISTENCY trained ResNet110 at  $\sigma_\epsilon = 0.25$ . We obtain up to 50-fold certification speed ups and 45-fold sample complexity reductions, while generally not incurring any accuracy penalties. For some radii, this makes certifying an ensemble with CERTIFYADP just as fast as certifying an individual model with CERTIFY. Comparing the sample complexity reduction factor of individual CONSISTENCY trained models (e.g., 30.17 for an at  $r = 0.25$ ), with that of an ensemble of 10 models (46.17, see Table 5), we observe that the adaptive sampling mechanism is particularly effective for ensembles, as their lower variance makes early decisions more likely. We observe that  $K$ -Consensus aggregation and adaptive sampling complement each other well: As the certification radius  $r$  increases and significantly more perturbations have to be evaluated as more samples pass on to the later stages of CERTIFYADP, KCR also rises making these evaluations cheaper.  $K$ -Consensus aggregation is more likely to trigger in this setting, as only samples with true underlying success probability close to the high required success probability reach the later phases before being certified or abstained from.

Both techniques are also applicable to ImageNet but due to the small ensemble size of just  $k = 3$  we chose to just use adaptive sampling and obtain up to 27-fold certification speed ups, making the evaluation of the full ensemble almost 10 times faster at some radii, than a standard certification of an individual model. See App. E.5 for more detailed results.



Table 4: Adaptive sampling for different  $\{n_j\}$  on CIFAR10 at  $\sigma_\epsilon = 0.25$ . SampleRF and TimeRF are the reduction factors in comparison to standard sampling with  $n = 100'000$  (larger is better).  $ASR_j$  is the portion of certification attempts returned in phase  $j$ .

$r$	Training	$\{n_j\}$	$acc_{cert}$ [%]	$ASR_1$ [%]	$ASR_2$ [%]	$ASR_3$ [%]	SampleRF	TimeRF
0.25	GAUSSIAN	1'000, 115'000	60.0	92.6	7.4	-	10.50	10.72
		10'000, 115'000	60.2	97.6	2.4	-	7.93	8.04
		1'000, 10'000, 125'000	60.2	90.6	6.0	3.4	17.09	16.37
	CONSISTENCY	1'000, 10'000, 125'000	66.0	95.8	2.6	1.6	<b>30.17</b>	<b>28.30</b>
0.75	GAUSSIAN	1'000, 10'000, 125'000	30.6	61.2	28.6	10.2	<b>6.13</b>	<b>5.82</b>
	CONSISTENCY	1'000, 10'000, 125'000	46.2	40.6	49.8	9.6	5.72	5.27

Table 5: Adaptive sampling ( $\{n_j\} = \{1'000, 10'000, 125'000\}$ ) and  $K$ -Consensus agg. ( $K = 6$ ) on CIFAR10 for 10 CONSISTENCY ResNet110. SampleRF and TimeRF are the reduction factors in comparison to standard sampling with  $n = 100'000$  (larger is better).  $ASR_j$  is the % of certification attempts returned in phase  $j$ . KCR is the % of inputs for which only  $K$  classifiers were evaluated.

Radius	$\sigma_\epsilon$	$acc_{cert}$ [%]	$ASR_1$ [%]	$ASR_2$ [%]	$ASR_3$ [%]	SampleRF	KCR [%]	TimeRF
0.25	0.25	70.4	95.8	3.6	0.6	<b>46.17</b>	50.7	<b>50.3</b>
0.50	0.25	60.4	90.8	6.2	3.0	18.61	55.2	20.4
0.75	0.25	52.0	36.4	55.4	8.2	6.16	84.8	7.9
1.00	0.50	38.6	89.2	7.2	3.6	16.11	73.4	20.0
1.25	0.50	32.2	54.4	40.4	5.2	8.95	89.7	12.2
1.50	0.50	26.2	60.2	31.4	8.4	6.98	<b>95.5</b>	9.9

**Denoised Smoothing** We show the general applicability of our ensembling approach, by applying it to the setting of denoised smoothing [45]. We consider 4 pretrained denoisers and combine them with a single standard ResNet110 (see App. D.3 for details). Comparing the strongest resulting model with an ensemble of all 4 at  $\sigma_\epsilon = 0.25$ , we observe an 17% ACR improvement. Training strong denoisers with current methods is challenging. However, based on these results we are confident that advances in denoiser training combined with ensembles can present an efficient way to obtain strong provable models.

Table 6: Denoised smoothing ensembles on CIFAR10 at  $\sigma_\epsilon = 0.25$

$k$	ACR	Radius $r$			
		0.0	0.25	0.50	0.75
1	0.378	<b>76.4</b>	56.6	36.8	19.2
4	<b>0.445</b>	75.2	<b>62.2</b>	<b>45.8</b>	<b>29.0</b>

**Limitations** Despite our significant improvements, certification and inference costs for RS remain high and are exacerbated by ensembles as base classifiers. This is especially pronounced when the target radius is not known a priori and adaptive sampling can not be applied. While we outperform large individual models with ensembles of smaller ones at lower total parameter count, training the diverse ensembles of large networks we use to obtain the new state-of-the-art results is computationally expensive. Further, for the ensembling approach to work well, networks have to be sufficiently diverse.

## 8 Conclusion

We propose a theoretically motivated and statistically sound approach to construct low variance base classifiers for Randomized Smoothing by ensembling. We show theoretically and empirically why this approach significantly increases certified accuracy resulting in state-of-the-art results. To offset the computational overhead of ensembles, we develop a generally applicable adaptive sampling mechanism, reducing certification costs up to 50-fold for predetermined radii and an ensemble aggregation mechanism, complementing it and reducing evaluation costs on its own up to 6-fold.

## 9 Societal Impact

Most machine learning techniques can be applied both in societally positive and negative ways. Techniques to increase the certified robustness of models do not change this, but only make the underlying models more robust, again allowing beneficial and malicious applications, e.g., more robust medical models versus more robust weaponized AI. As our contributions improve certified accuracy, certification radii and inference speed both of these facets of robust AI are amplified. Furthermore, while we achieve state-of-the-art results, these do not yet extend to realistic perturbations. Malicious actors may aim to convince regulators that methods such as the proposed approach are sufficient to provide guarantees for general real-world threat scenarios, leading to insufficient safeguards.

## References

- [1] Battista Biggio, Igino Corona, Davide Maiorca, Blaine Nelson, Nedim Srndic, Pavel Laskov, Giorgio Giacinto, and Fabio Roli. Evasion attacks against machine learning at test time. In Hendrik Blockeel, Kristian Kersting, Siegfried Nijssen, and Filip Zelezný, editors, *Machine Learning and Knowledge Discovery in Databases - European Conference, ECML PKDD 2013, Prague, Czech Republic, September 23-27, 2013, Proceedings, Part III*, volume 8190 of *Lecture Notes in Computer Science*, pages 387–402. Springer, 2013. doi: 10.1007/978-3-642-40994-3\_25. URL [https://doi.org/10.1007/978-3-642-40994-3\\_25](https://doi.org/10.1007/978-3-642-40994-3_25).
- [2] Christian Szegedy, Wojciech Zaremba, Ilya Sutskever, Joan Bruna, Dumitru Erhan, Ian J. Goodfellow, and Rob Fergus. Intriguing properties of neural networks. In Yoshua Bengio and Yann LeCun, editors, *2nd International Conference on Learning Representations, ICLR 2014, Banff, AB, Canada, April 14-16, 2014, Conference Track Proceedings*, 2014. URL <http://arxiv.org/abs/1312.6199>.
- [3] Florian Tramèr, Nicholas Carlini, Wieland Brendel, and Aleksander Madry. On adaptive attacks to adversarial example defenses. In Hugo Larochelle, Marc’Aurelio Ranzato, Raia Hadsell, Maria-Florina Balcan, and Hsuan-Tien Lin, editors, *Advances in Neural Information Processing Systems 33: Annual Conference on Neural Information Processing Systems 2020, NeurIPS 2020, December 6-12, 2020, virtual*, 2020. URL <https://proceedings.neurips.cc/paper/2020/hash/11f38f8ecd71867b42433548d1078e38-Abstract.html>.
- [4] Nicholas Carlini and David A. Wagner. Towards evaluating the robustness of neural networks. In *2017 IEEE Symposium on Security and Privacy, SP 2017, San Jose, CA, USA, May 22-26, 2017*, pages 39–57. IEEE Computer Society, 2017. doi: 10.1109/SP.2017.49. URL <https://doi.org/10.1109/SP.2017.49>.
- [5] Jeremy M. Cohen, Elan Rosenfeld, and J. Zico Kolter. Certified adversarial robustness via randomized smoothing. In Kamalika Chaudhuri and Ruslan Salakhutdinov, editors, *Proceedings of the 36th International Conference on Machine Learning, ICML 2019, 9-15 June 2019, Long Beach, California, USA*, volume 97 of *Proceedings of Machine Learning Research*, pages 1310–1320. PMLR, 2019. URL <http://proceedings.mlr.press/v97/cohen19c.html>.
- [6] Hadi Salman, Jerry Li, Ilya P. Razenshteyn, Pengchuan Zhang, Huan Zhang, Sébastien Bubeck, and Greg Yang. Provably robust deep learning via adversarially trained smoothed classifiers. In Hanna M. Wallach, Hugo Larochelle, Alina Beygelzimer, Florence d’Alché-Buc, Emily B. Fox, and Roman Garnett, editors, *Advances in Neural Information Processing Systems 32: Annual Conference on Neural Information Processing Systems 2019, NeurIPS 2019, December 8-14, 2019, Vancouver, BC, Canada*, pages 11289–11300, 2019. URL <https://proceedings.neurips.cc/paper/2019/hash/3a24b25a7b092a252166a1641ae953e7-Abstract.html>.
- [7] Runtian Zhai, Chen Dan, Di He, Huan Zhang, Boqing Gong, Pradeep Ravikumar, Cho-Jui Hsieh, and Liwei Wang. MACER: attack-free and scalable robust training via maximizing certified radius. In *8th International Conference on Learning Representations, ICLR 2020, Addis Ababa, Ethiopia, April 26-30, 2020*. OpenReview.net, 2020. URL <https://openreview.net/forum?id=rJx1Na4Fwr>.
- [8] Jongheon Jeong and Jinwoo Shin. Consistency regularization for certified robustness of smoothed classifiers. In Hugo Larochelle, Marc’Aurelio Ranzato, Raia Hadsell, Maria-Florina Balcan, and Hsuan-Tien Lin, editors, *Advances in Neural Information Processing Systems 33: Annual Conference on Neural Information Processing Systems 2020, NeurIPS 2020, December 6-12, 2020, virtual*, 2020. URL <https://proceedings.neurips.cc/paper/2020/hash/77330e1330ae2b086e5bfcae50d9ffae-Abstract.html>.
- [9] Lars Kai Hansen and Peter Salamon. Neural network ensembles. *IEEE Trans. Pattern Anal. Mach. Intell.*, 12(10):993–1001, 1990. doi: 10.1109/34.58871. URL <https://doi.org/10.1109/34.58871>.
- [10] Kaiming He, Xiangyu Zhang, Shaoqing Ren, and Jian Sun. Deep residual learning for image recognition. In *2016 IEEE Conference on Computer Vision and Pattern Recognition, CVPR 2016, Las Vegas, NV, USA, June 27-30, 2016*, pages 770–778. IEEE Computer Society, 2016. doi: 10.1109/CVPR.2016.90. URL <https://doi.org/10.1109/CVPR.2016.90>.

- [11] Gao Huang, Zhuang Liu, Laurens van der Maaten, and Kilian Q. Weinberger. Densely connected convolutional networks. In *2017 IEEE Conference on Computer Vision and Pattern Recognition, CVPR 2017, Honolulu, HI, USA, July 21-26, 2017*, pages 2261–2269. IEEE Computer Society, 2017. doi: 10.1109/CVPR.2017.243. URL <https://doi.org/10.1109/CVPR.2017.243>.
- [12] Abdul Wasay and Stratos Idreos. More or less: When and how to build convolutional neural network ensembles. In *International Conference on Learning Representations*, 2021. URL <https://openreview.net/forum?id=z5Z023VBmDZ>.
- [13] Alexey Kurakin, Ian J. Goodfellow, and Samy Bengio. Adversarial machine learning at scale. In *5th International Conference on Learning Representations, ICLR 2017, Toulon, France, April 24-26, 2017, Conference Track Proceedings*. OpenReview.net, 2017. URL <https://openreview.net/forum?id=BJm4T4Kgx>.
- [14] Aleksander Madry, Aleksandar Makelov, Ludwig Schmidt, Dimitris Tsipras, and Adrian Vladu. Towards deep learning models resistant to adversarial attacks. In *6th International Conference on Learning Representations, ICLR 2018, Vancouver, BC, Canada, April 30 - May 3, 2018, Conference Track Proceedings*. OpenReview.net, 2018. URL <https://openreview.net/forum?id=rJzIBfZAb>.
- [15] Timon Gehr, Matthew Mirman, Dana Drachler-Cohen, Petar Tsankov, Swarat Chaudhuri, and Martin T. Vechev. AI2: safety and robustness certification of neural networks with abstract interpretation. In *2018 IEEE Symposium on Security and Privacy, SP 2018, Proceedings, 21-23 May 2018, San Francisco, California, USA*, pages 3–18. IEEE Computer Society, 2018. doi: 10.1109/SP.2018.00058. URL <https://doi.org/10.1109/SP.2018.00058>.
- [16] Huan Zhang, Tsui-Wei Weng, Pin-Yu Chen, Cho-Jui Hsieh, and Luca Daniel. Efficient neural network robustness certification with general activation functions. In Samy Bengio, Hanna M. Wallach, Hugo Larochelle, Kristen Grauman, Nicolò Cesa-Bianchi, and Roman Garnett, editors, *Advances in Neural Information Processing Systems 31: Annual Conference on Neural Information Processing Systems 2018, NeurIPS 2018, December 3-8, 2018, Montréal, Canada*, pages 4944–4953, 2018. URL <https://proceedings.neurips.cc/paper/2018/hash/d04863f100d59b3eb688a11f95b0ae60-Abstract.html>.
- [17] Shiqi Wang, Kexin Pei, Justin Whitehouse, Junfeng Yang, and Suman Jana. Efficient formal safety analysis of neural networks. In Samy Bengio, Hanna M. Wallach, Hugo Larochelle, Kristen Grauman, Nicolò Cesa-Bianchi, and Roman Garnett, editors, *Advances in Neural Information Processing Systems 31: Annual Conference on Neural Information Processing Systems 2018, NeurIPS 2018, December 3-8, 2018, Montréal, Canada*, pages 6369–6379, 2018. URL <https://proceedings.neurips.cc/paper/2018/hash/2ecd2bd94734e5dd392d8678bc64cdab-Abstract.html>.
- [18] Tsui-Wei Weng, Huan Zhang, Hongge Chen, Zhao Song, Cho-Jui Hsieh, Luca Daniel, Duane S. Boning, and Inderjit S. Dhillon. Towards fast computation of certified robustness for relu networks. In Jennifer G. Dy and Andreas Krause, editors, *Proceedings of the 35th International Conference on Machine Learning, ICML 2018, Stockholmsmässan, Stockholm, Sweden, July 10-15, 2018*, volume 80 of *Proceedings of Machine Learning Research*, pages 5273–5282. PMLR, 2018. URL <http://proceedings.mlr.press/v80/weng18a.html>.
- [19] Eric Wong and J. Zico Kolter. Provable defenses against adversarial examples via the convex outer adversarial polytope. In Jennifer G. Dy and Andreas Krause, editors, *Proceedings of the 35th International Conference on Machine Learning, ICML 2018, Stockholmsmässan, Stockholm, Sweden, July 10-15, 2018*, volume 80 of *Proceedings of Machine Learning Research*, pages 5283–5292. PMLR, 2018. URL <http://proceedings.mlr.press/v80/wong18a.html>.
- [20] Gagandeep Singh, Timon Gehr, Matthew Mirman, Markus Püschel, and Martin T. Vechev. Fast and effective robustness certification. In Samy Bengio, Hanna M. Wallach, Hugo Larochelle, Kristen Grauman, Nicolò Cesa-Bianchi, and Roman Garnett, editors, *Advances in Neural Information Processing Systems 31: Annual Conference on Neural Information Processing Systems 2018, NeurIPS 2018, December 3-8, 2018, Montréal, Canada*, pages 10825–10836, 2018. URL <https://proceedings.neurips.cc/paper/2018/hash/f2f446980d8e971ef3da97af089481c3-Abstract.html>.

- [21] Gagandeep Singh, Timon Gehr, Markus Püschel, and Martin T. Vechev. An abstract domain for certifying neural networks. *Proc. ACM Program. Lang.*, 3(POPL):41:1–41:30, 2019. doi: 10.1145/3290354. URL <https://doi.org/10.1145/3290354>.
- [22] Kaidi Xu, Zhouxing Shi, Huan Zhang, Yihan Wang, Kai-Wei Chang, Minlie Huang, Bhavya Kailkhura, Xue Lin, and Cho-Jui Hsieh. Automatic perturbation analysis for scalable certified robustness and beyond. In Hugo Larochelle, Marc’Aurelio Ranzato, Raia Hadsell, Maria-Florina Balcan, and Hsuan-Tien Lin, editors, *Advances in Neural Information Processing Systems 33: Annual Conference on Neural Information Processing Systems 2020, NeurIPS 2020, December 6-12, 2020, virtual*, 2020. URL <https://proceedings.neurips.cc/paper/2020/hash/0cbc5671ae26f67871cb914d81ef8fc1-Abstract.html>.
- [23] Mark Niklas Müller, Gleb Makarchuk, Gagandeep Singh, Markus Püschel, and Martin Vechev. Prima: Precise and general neural network certification via multi-neuron convex relaxations. *arXiv preprint arXiv:2103.03638*, 2021.
- [24] Vincent Tjeng, Kai Y. Xiao, and Russ Tedrake. Evaluating robustness of neural networks with mixed integer programming. 2019. URL <https://openreview.net/forum?id=HyGIIdRqtm>.
- [25] Aditi Raghunathan, Jacob Steinhardt, and Percy Liang. Semidefinite relaxations for certifying robustness to adversarial examples. In Samy Bengio, Hanna M. Wallach, Hugo Larochelle, Kristen Grauman, Nicolò Cesa-Bianchi, and Roman Garnett, editors, *Advances in Neural Information Processing Systems 31: Annual Conference on Neural Information Processing Systems 2018, NeurIPS 2018, December 3-8, 2018, Montréal, Canada*, pages 10900–10910, 2018. URL <https://proceedings.neurips.cc/paper/2018/hash/29c0605a3bab4229e46723f89cf59d83-Abstract.html>.
- [26] Sumanth Dathathri, Krishnamurthy Dvijotham, Alexey Kurakin, Aditi Raghunathan, Jonathan Uesato, Rudy Bunel, Shreya Shankar, Jacob Steinhardt, Ian J. Goodfellow, Percy Liang, and Pushmeet Kohli. Enabling certification of verification-agnostic networks via memory-efficient semidefinite programming. In Hugo Larochelle, Marc’Aurelio Ranzato, Raia Hadsell, Maria-Florina Balcan, and Hsuan-Tien Lin, editors, *Advances in Neural Information Processing Systems 33: Annual Conference on Neural Information Processing Systems 2020, NeurIPS 2020, December 6-12, 2020, virtual*, 2020. URL <https://proceedings.neurips.cc/paper/2020/hash/397d6b4c83c91021fe928a8c4220386b-Abstract.html>.
- [27] Guy Katz, Clark W. Barrett, David L. Dill, Kyle Julian, and Mykel J. Kochenderfer. Reluplex: An efficient SMT solver for verifying deep neural networks. In Rupak Majumdar and Viktor Kuncak, editors, *Computer Aided Verification - 29th International Conference, CAV 2017, Heidelberg, Germany, July 24-28, 2017, Proceedings, Part I*, volume 10426 of *Lecture Notes in Computer Science*, pages 97–117. Springer, 2017. doi: 10.1007/978-3-319-63387-9\_5. URL [https://doi.org/10.1007/978-3-319-63387-9\\_5](https://doi.org/10.1007/978-3-319-63387-9_5).
- [28] Rüdiger Ehlers. Formal verification of piece-wise linear feed-forward neural networks. In Deepak D’Souza and K. Narayan Kumar, editors, *Automated Technology for Verification and Analysis - 15th International Symposium, ATVA 2017, Pune, India, October 3-6, 2017, Proceedings*, volume 10482 of *Lecture Notes in Computer Science*, pages 269–286. Springer, 2017. doi: 10.1007/978-3-319-68167-2\_19. URL [https://doi.org/10.1007/978-3-319-68167-2\\_19](https://doi.org/10.1007/978-3-319-68167-2_19).
- [29] Aditi Raghunathan, Jacob Steinhardt, and Percy Liang. Certified defenses against adversarial examples. In *6th International Conference on Learning Representations, ICLR 2018, Vancouver, BC, Canada, April 30 - May 3, 2018, Conference Track Proceedings*. OpenReview.net, 2018. URL <https://openreview.net/forum?id=Bys4ob-Rb>.
- [30] Matthew Mirman, Timon Gehr, and Martin T. Vechev. Differentiable abstract interpretation for provably robust neural networks. In Jennifer G. Dy and Andreas Krause, editors, *Proceedings of the 35th International Conference on Machine Learning, ICML 2018, Stockholm, Sweden, July 10-15, 2018*, volume 80 of *Proceedings of Machine Learning Research*, pages 3575–3583. PMLR, 2018. URL <http://proceedings.mlr.press/v80/mirman18b.html>.

- [31] Sven Gowal, Krishnamurthy Dvijotham, Robert Stanforth, Rudy Bunel, Chongli Qin, Jonathan Uesato, Relja Arandjelovic, Timothy A. Mann, and Pushmeet Kohli. On the effectiveness of interval bound propagation for training verifiably robust models. *CoRR*, abs/1810.12715, 2018. URL <http://arxiv.org/abs/1810.12715>.
- [32] Mislav Balunovic and Martin T. Vechev. Adversarial training and provable defenses: Bridging the gap. In *8th International Conference on Learning Representations, ICLR 2020, Addis Ababa, Ethiopia, April 26-30, 2020*. OpenReview.net, 2020. URL <https://openreview.net/forum?id=SJxSDxrKDr>.
- [33] Bai Li, Changyou Chen, Wenlin Wang, and Lawrence Carin. Certified adversarial robustness with additive noise. In Hanna M. Wallach, Hugo Larochelle, Alina Beygelzimer, Florence d’Alché-Buc, Emily B. Fox, and Roman Garnett, editors, *Advances in Neural Information Processing Systems 32: Annual Conference on Neural Information Processing Systems 2019, NeurIPS 2019, December 8-14, 2019, Vancouver, BC, Canada*, pages 9459–9469, 2019. URL <https://proceedings.neurips.cc/paper/2019/hash/335cd1b90bfa4ee70b39d08a4ae0cf2d-Abstract.html>.
- [34] Mathias Lécuyer, Vaggelis Atlidakis, Roxana Geambasu, Daniel Hsu, and Suman Jana. Certified robustness to adversarial examples with differential privacy. In *2019 IEEE Symposium on Security and Privacy, SP 2019, San Francisco, CA, USA, May 19-23, 2019*, pages 656–672. IEEE, 2019. doi: 10.1109/SP.2019.00044. URL <https://doi.org/10.1109/SP.2019.00044>.
- [35] Greg Yang, Tony Duan, J. Edward Hu, Hadi Salman, Ilya P. Razenshteyn, and Jerry Li. Randomized smoothing of all shapes and sizes. In *Proceedings of the 37th International Conference on Machine Learning, ICML 2020, 13-18 July 2020, Virtual Event, 2020*.
- [36] Krishnamurthy (Dj) Dvijotham, Jamie Hayes, Borja Balle, J. Zico Kolter, Chongli Qin, András György, Kai Xiao, Sven Gowal, and Pushmeet Kohli. A framework for robustness certification of smoothed classifiers using f-divergences. In *8th International Conference on Learning Representations, ICLR 2020, Addis Ababa, Ethiopia, April 26-30, 2020, 2020*.
- [37] Hongbin Liu, Jinyuan Jia, and Neil Zhenqiang Gong. Pointguard: Provably robust 3d point cloud classification. *arXiv preprint arXiv:2103.03046*, 2021.
- [38] Alexander Levine and Soheil Feizi. Robustness certificates for sparse adversarial attacks by randomized ablation. In *The Thirty-Fourth AAAI Conference on Artificial Intelligence, AAAI 2020, The Thirty-Second Innovative Applications of Artificial Intelligence Conference, IAAI 2020, The Tenth AAAI Symposium on Educational Advances in Artificial Intelligence, EAAI 2020, New York, NY, USA, February 7-12, 2020, 2020*.
- [39] Alexander Levine and Soheil Feizi. (de)randomized smoothing for certifiable defense against patch attacks. In *Advances in Neural Information Processing Systems 33: Annual Conference on Neural Information Processing Systems 2020, NeurIPS 2020, December 6-12, 2020, virtual, 2020*.
- [40] Jinyuan Jia, Binghui Wang, Xiaoyu Cao, and Neil Zhenqiang Gong. Certified robustness of community detection against adversarial structural perturbation via randomized smoothing. In *WWW ’20: The Web Conference 2020, Taipei, Taiwan, April 20-24, 2020, 2020*.
- [41] Aleksandar Bojchevski, Johannes Klicpera, and Stephan Günnemann. Efficient robustness certificates for discrete data: Sparsity-aware randomized smoothing for graphs, images and more. In *Proceedings of the 37th International Conference on Machine Learning, ICML 2020, 13-18 July 2020, Virtual Event, 2020*.
- [42] Guang-He Lee, Yang Yuan, Shiyu Chang, and Tommi S. Jaakkola. Tight certificates of adversarial robustness for randomly smoothed classifiers. In *Advances in Neural Information Processing Systems 32: Annual Conference on Neural Information Processing Systems 2019, NeurIPS 2019, December 8-14, 2019, Vancouver, BC, Canada, 2019*.
- [43] Marc Fischer, Maximilian Baader, and Martin T. Vechev. Certified defense to image transformations via randomized smoothing. In *Advances in Neural Information Processing Systems 33: Annual Conference on Neural Information Processing Systems 2020, NeurIPS 2020, December 6-12, 2020, virtual, 2020*.

- [44] Jan Schuchardt, Aleksandar Bojchevski, Johannes Klicpera, and Stephan Günnemann. Collective robustness certificates. In *International Conference on Learning Representations*, 2021. URL <https://openreview.net/forum?id=ULQdiUTHe3y>.
- [45] Hadi Salman, Mingjie Sun, Greg Yang, Ashish Kapoor, and J. Zico Kolter. Denoised smoothing: A provable defense for pretrained classifiers. In Hugo Larochelle, Marc Aurelio Ranzato, Raia Hadsell, Maria-Florina Balcan, and Hsuan-Tien Lin, editors, *Advances in Neural Information Processing Systems 33: Annual Conference on Neural Information Processing Systems 2020, NeurIPS 2020, December 6-12, 2020, virtual*, 2020. URL <https://proceedings.neurips.cc/paper/2020/hash/f9fd2624beefbc7808e4e405d73f57ab-Abstract.html>.
- [46] Josef Kittler, Mohamad Hatef, Robert P. W. Duin, and Jiri Matas. On combining classifiers. *IEEE Trans. Pattern Anal. Mach. Intell.*, 20(3):226–239, 1998. doi: 10.1109/34.667881. URL <https://doi.org/10.1109/34.667881>.
- [47] Hiroshi Inoue. Adaptive ensemble prediction for deep neural networks based on confidence level. In Kamalika Chaudhuri and Masashi Sugiyama, editors, *The 22nd International Conference on Artificial Intelligence and Statistics, AISTATS 2019, 16-18 April 2019, Naha, Okinawa, Japan*, volume 89 of *Proceedings of Machine Learning Research*, pages 1284–1293. PMLR, 2019. URL <http://proceedings.mlr.press/v89/inoue19a.html>.
- [48] Thomas G. Dietterich. Ensemble methods in machine learning. In Josef Kittler and Fabio Roli, editors, *Multiple Classifier Systems, First International Workshop, MCS 2000, Cagliari, Italy, June 21-23, 2000, Proceedings*, volume 1857 of *Lecture Notes in Computer Science*, pages 1–15. Springer, 2000. doi: 10.1007/3-540-45014-9\_1. URL [https://doi.org/10.1007/3-540-45014-9\\_1](https://doi.org/10.1007/3-540-45014-9_1).
- [49] Kagan Tumer and Joydeep Ghosh. Analysis of decision boundaries in linearly combined neural classifiers. *Pattern recognition*, 29(2):341–348, 1996.
- [50] Kagan Tumer and Joydeep Ghosh. Error correlation and error reduction in ensemble classifiers. *Connect. Sci.*, 8(3):385–404, 1996. doi: 10.1080/095400996116839. URL <https://doi.org/10.1080/095400996116839>.
- [51] Chizhou Liu, Yunzhen Feng, Ranran Wang, and Bin Dong. Enhancing certified robustness of smoothed classifiers via weighted model ensembling. *CoRR*, abs/2005.09363, 2020. URL <https://arxiv.org/abs/2005.09363>.
- [52] Ruoxi Qin, Linyuan Wang, Xingyuan Chen, Xuehui Du, and Bin Yan. Dynamic defense approach for adversarial robustness in deep neural networks via stochastic ensemble smoothed model. *CoRR*, abs/2105.02803, 2021. URL <https://arxiv.org/abs/2105.02803>.
- [53] C. J. Clopper and E. S. Pearson. The use of confidence or fiducial limits illustrated in the case of the binomial. *Biometrika*, 26(4):404–413, 1934. ISSN 00063444. URL <http://www.jstor.org/stable/2331986>.
- [54] Serena Wang, Maya R. Gupta, and Seungil You. Quit when you can: Efficient evaluation of ensembles with ordering optimization. *CoRR*, abs/1806.11202, 2018. URL <http://arxiv.org/abs/1806.11202>.
- [55] Víctor Soto, Alberto Suárez, and Gonzalo Martínez-Muñoz. An urn model for majority voting in classification ensembles. In Daniel D. Lee, Masashi Sugiyama, Ulrike von Luxburg, Isabelle Guyon, and Roman Garnett, editors, *Advances in Neural Information Processing Systems 29: Annual Conference on Neural Information Processing Systems 2016, December 5-10, 2016, Barcelona, Spain*, pages 4430–4438, 2016. URL <https://proceedings.neurips.cc/paper/2016/hash/d1a21da7bca4abff8b0b61b87597de73-Abstract.html>.
- [56] Alex Krizhevsky, Geoffrey Hinton, et al. Learning multiple layers of features from tiny images. 2009.
- [57] Olga Russakovsky, Jia Deng, Hao Su, Jonathan Krause, Sanjeev Satheesh, Sean Ma, Zhiheng Huang, Andrej Karpathy, Aditya Khosla, Michael Bernstein, Alexander C. Berg, and Li Fei-Fei. ImageNet Large Scale Visual Recognition Challenge. *International Journal of Computer Vision (IJCV)*, 115(3):211–252, 2015. doi: 10.1007/s11263-015-0816-y.

- [58] Adam Paszke, Sam Gross, Francisco Massa, Adam Lerer, James Bradbury, Gregory Chanan, Trevor Killeen, Zeming Lin, Natalia Gimelshein, Luca Antiga, Alban Desmaison, Andreas Köpf, Edward Yang, Zachary DeVito, Martin Raison, Alykhan Tejani, Sasank Chilamkurthy, Benoit Steiner, Lu Fang, Junjie Bai, and Soumith Chintala. Pytorch: An imperative style, high-performance deep learning library. In Hanna M. Wallach, Hugo Larochelle, Alina Beygelzimer, Florence d'Alché-Buc, Emily B. Fox, and Roman Garnett, editors, *Advances in Neural Information Processing Systems 32: Annual Conference on Neural Information Processing Systems 2019, NeurIPS 2019, December 8-14, 2019, Vancouver, BC, Canada*, pages 8024–8035, 2019. URL <https://proceedings.neurips.cc/paper/2019/hash/bdbca288fee7f92f2bfa9f7012727740-Abstract.html>.
- [59] Carlo Bonferroni. Teoria statistica delle classi e calcolo delle probabilita. *Pubblicazioni del R Istituto Superiore di Scienze Economiche e Commerciali di Firenze*, 8:3–62, 1936.
- [60] Jérôme Rony, Luiz G. Hafemann, Luiz S. Oliveira, Ismail Ben Ayed, Robert Sabourin, and Eric Granger. Decoupling direction and norm for efficient gradient-based L2 adversarial attacks and defenses. In *IEEE Conference on Computer Vision and Pattern Recognition, CVPR 2019, Long Beach, CA, USA, June 16-20, 2019*, pages 4322–4330. Computer Vision Foundation / IEEE, 2019. doi: 10.1109/CVPR.2019.00445. URL [http://openaccess.thecvf.com/content\\_CVPR\\_2019/html/Rony-Decoupling\\_Direction\\_and\\_Norm\\_for\\_Efficient\\_Gradient-Based\\_L2\\_Adversarial\\_Attacks\\_CVPR\\_2019\\_paper.html](http://openaccess.thecvf.com/content_CVPR_2019/html/Rony-Decoupling_Direction_and_Norm_for_Efficient_Gradient-Based_L2_Adversarial_Attacks_CVPR_2019_paper.html).

## A Comparison to Liu et al. [51]

Liu et al. [51] introduce Smoothed Weighted Ensembling (SWEEN), which are weighted ensembles of smoothed base models. They focus on deriving optimal ensemble weights for generalization rather than on analyzing the particularities of ensembles in the RS setting. As they do not consider multiple testing correction and the confidence of the applied Monte Carlo sampling they obtain statements about empirical, distributional robustness of their classifiers, rather than individual certificates with high confidence. Due to this difference in setting we do not compare numerically.

## B Mathematical Derivation of Variance Reduction for Ensembles

In this section, we present the algebraic derivations for §5, skipped in the main part due to space constraints.

**Individual Classifier** In §5 define  $f^l(\mathbf{x}) =: \mathbf{y}^l \in \mathbb{R}^m$  as the sum of two random variables  $\mathbf{y}^l = \mathbf{y}_p^l + \mathbf{y}_c^l$ .

The behaviour on a specific clean sample  $\mathbf{x}$  is modeled by  $\mathbf{y}_c^l$  with mean  $\mathbf{c} \in \mathbb{R}^m$ , the expectation of the logits for this sample over the randomization in the training process, and corresponding covariance  $\Sigma_c$ :

$$\begin{aligned}\mathbb{E}[\mathbf{y}_c^l] &= \mathbf{c} \\ \text{Cov}[\mathbf{y}_c^l] &= \Sigma_c = \begin{bmatrix} \sigma_{c,1}^2 & \cdots & \rho_{c,1m}\sigma_{c,1}\sigma_{c,m} \\ & \ddots & \vdots \\ & & \sigma_{c,m}^2 \end{bmatrix}\end{aligned}$$

We note that: (i) we omit the lower triangular part of covariance matrices due to symmetry, (ii)  $\mathbf{c}$  and  $\Sigma_c$  are constant across the different  $f^l$  for a fixed  $\mathbf{x}$  and (iii) that due to (ii) and our modelling assumptions all means, (co)variances and probabilities are conditioned on  $\mathbf{x}$ , e.g.,  $\mathbb{E}[\mathbf{y}_c^l] = \mathbb{E}[\mathbf{y}_c^l | \mathbf{x}] = \mathbf{c}$ . However, as we define all random variables only for a fixed  $\mathbf{x}$  we omit this.

Similarly, we model the impact of the perturbations  $\epsilon$  introduced during RS by  $\mathbf{y}_p^l$  with mean zero and covariance  $\Sigma_p$ :

$$\begin{aligned}\mathbb{E}[\mathbf{y}_p^l] &= \mathbf{0} \\ \text{Cov}[\mathbf{y}_p^l] &= \Sigma_p = \begin{bmatrix} \sigma_{p,1}^2 & \cdots & \rho_{p,1m}\sigma_{p,1}\sigma_{p,m} \\ & \ddots & \vdots \\ & & \sigma_{p,m}^2 \end{bmatrix}\end{aligned}$$

That is, we assume  $\mathbf{c}^l$  to be the expected classification a model learns for the clean sample while the covariances  $\Sigma_c$  and  $\Sigma_p$  encode the stochasticity of the training process and perturbations respectively. As  $\mathbf{y}_p^l$  models the local behaviour under small perturbations and  $\mathbf{y}_c^l$  models the global training effects, we assume them to be independent:

$$\begin{aligned}\mathbb{E}[\mathbf{y}^l] &= \mathbf{c} \\ \text{Cov}[\mathbf{y}^l] &= \Sigma = \Sigma_c + \Sigma_p = \begin{bmatrix} \sigma_{p,1}^2 + \sigma_{c,1}^2 & \cdots & \rho_{p,1m}\sigma_{p,1}\sigma_{p,m} + \rho_{c,1m}\sigma_{c,1}\sigma_{c,m} \\ & \ddots & \vdots \\ & & \sigma_{p,m}^2 + \sigma_{c,m}^2 \end{bmatrix}.\end{aligned}$$

The classifier prediction  $\arg \max_q y_q$  is determined by the differences between logits. We call the difference between the target logit and others the classification margin. During certification with RS, the first step is to determine the majority class. Without loss of generality, we will in the following assume, that it has been determined to index 1 leading to the classification margin,  $z_i = y_1 - y_i$ . If  $z_i > 0$  for all  $i \neq 1$ , the majority class logit  $y_1$  is larger than those of all other classes  $y_i$ . We define  $\mathbf{z} := [z_2, \dots, z_n]^T$ , skipping the margin of  $y_1$  to itself. Under the above assumptions, the statistics of the classification margin for a single classifier are:

$$\begin{aligned}\mathbb{E}[z_i] &= c_1 - c_i \\ \text{Var}[z_i] &= \sigma_{p,1}^2 + \sigma_{p,i}^2 + \sigma_{c,1}^2 + \sigma_{c,i}^2 - 2\rho_{p,1i}\sigma_{p,1}\sigma_{p,i} - 2\rho_{c,1i}\sigma_{c,1}\sigma_{c,i}\end{aligned}$$



**Ensemble** Now, we construct an ensemble of  $k$  of these classifiers. Using soft-voting (cf. Eq. (2)) to compute the ensemble output  $\bar{\mathbf{y}} = \frac{1}{k} \sum_{l=1}^k \mathbf{y}^l$ . We assume the  $\mathbf{y}_p^i$  and  $\mathbf{y}_p^j$  to be correlated with  $\zeta_p \Sigma_p$  for classifiers  $i \neq j$  and similarly model the correlation of  $\mathbf{y}_c^l$  with  $\zeta_c \Sigma_c$  for  $\zeta_p, \zeta_c \in [-1, 1]$ . Letting  $\mathbf{y}^* := [\mathbf{y}^{1^\top}, \dots, \mathbf{y}^{k^\top}]^\top$  denote the concatenation of the logit vectors of all classifiers we assemble their joint covariance matrix in a block-wise manner from the classifier individual covariance matrices as:

$$\text{Cov}[\mathbf{y}^*] = \Sigma^* = \begin{bmatrix} \Sigma_p + \Sigma_c & \cdots & \zeta_p \Sigma_p + \zeta_c \Sigma_c \\ & \ddots & \vdots \\ & & \Sigma_p + \Sigma_c \end{bmatrix}$$

We then write the corresponding classification margins  $\bar{z}_i = \bar{y}_1 - \bar{y}_i$ . or in vector notation  $\bar{\mathbf{z}} := [\bar{z}_2, \dots, \bar{z}_n]^\top$ , again skipping the margin of  $\bar{y}_1$  to itself. By linearity of expectation we obtain  $\mathbb{E}[\bar{z}_i] = \mathbb{E}[z_i] = c_1 - c_i$  or equivalently

$$\mathbb{E}[\bar{\mathbf{z}}] = \bar{\boldsymbol{\mu}} = \begin{pmatrix} c_1 \\ \vdots \\ c_1 \end{pmatrix} - \mathbf{c}_{[2:n]}.$$

We define the ensemble difference matrix  $\mathbf{D} \in \mathbb{R}^{m-1 \times mk}$  with elements  $d_{i,j}$  such that  $\bar{\mathbf{z}} = \mathbf{D}\mathbf{y}^*$ :

$$D_{ij} = \begin{cases} \frac{1}{k}, & \text{if } j \bmod n = 1 \\ \frac{-1}{k}, & \text{else if } j \bmod n = i \bmod n, \quad j \in [1, \dots, nk], i \in [2, \dots, n]. \\ 0, & \text{else} \end{cases}$$

This allows us to write the covariance matrix of the ensemble classification margins

$$\text{Cov}[\bar{\mathbf{z}}] = \bar{\Sigma} = \mathbf{D}\Sigma^*\mathbf{D}^\top.$$

Now we can evaluate its diagonal elements or use the multinomial theorem and rule on the variance of correlated sums to obtain the variance of individual terms:

$$\text{Var}[\bar{z}_i] = \underbrace{\frac{k + 2\binom{k}{2}\zeta_p}{k^2}(\sigma_{p,1}^2 + \sigma_{p,i}^2 - 2\rho_{p,1i}\sigma_{p,1}\sigma_{p,i})}_{\sigma_p^2(k)} + \underbrace{\frac{k + 2\binom{k}{2}\zeta_c}{k^2}(\sigma_{c,1}^2 + \sigma_{c,i}^2 - 2\rho_{c,1i}\sigma_{c,1}\sigma_{c,i})}_{\sigma_c^2(k)}.$$

**Variance Reduction** We can split  $\text{Var}[\bar{z}_i]$  into the components associated with the perturbation effect  $\sigma_p^2(k)$  and the clean prediction  $\sigma_c^2(k)$ , all as functions of the ensemble element number  $k$ .

Now, we analyze these variance components independently, by normalizing them with the corresponding components of an individual classifier:

$$\begin{aligned} \frac{\sigma_p^2(k)}{\sigma_p^2(1)} &= \frac{(1 + \zeta_p(k-1))(\sigma_{p,1}^2 + \sigma_{p,i}^2 - 2\rho_{p,1i}\sigma_{p,1}\sigma_{p,i})}{k(\sigma_{p,1}^2 + \sigma_{p,i}^2 - 2\rho_{p,1i}\sigma_{p,1}\sigma_{p,i})} = \frac{1 + \zeta_p(k-1)}{k} \xrightarrow{k \rightarrow \infty} \zeta_p \\ \frac{\sigma_c^2(k)}{\sigma_c^2(1)} &= \frac{(1 + \zeta_c(k-1))(\sigma_{c,1}^2 + \sigma_{c,i}^2 - 2\rho_{c,1i}\sigma_{c,1}\sigma_{c,i})}{k(\sigma_{c,1}^2 + \sigma_{c,i}^2 - 2\rho_{c,1i}\sigma_{c,1}\sigma_{c,i})} = \frac{1 + \zeta_c(k-1)}{k} \xrightarrow{k \rightarrow \infty} \zeta_c \end{aligned}$$

We observe that both variance components go towards their corresponding correlation coefficients  $\zeta_p$  and  $\zeta_c$  as ensemble size grows, highlighting the importance of diverse classifiers.

Especially for samples that are near a decision boundary, this variance reduction will lead to much more consistent predictions, in turn significantly increasing the lower confidence bound  $\underline{p}_1$  and thereby the certified radius as per Theorem 3.1.

**Gaussian Perturbation Error** To calculate the improvement in success probability and consequently certified radius, we assume that both  $\mathbf{y}_p$  and  $\mathbf{y}_c$  follow multivariate normal distributions with  $\mathbf{y}_p^l \sim \mathcal{N}(\mathbf{0}, \Sigma_p)$  and  $\mathbf{y}_c^l \sim \mathcal{N}(\mathbf{c}, \Sigma_c)$ . As input perturbations follow a multivariate normal distributions such a distribution of  $\mathbf{y}_p$  follows directly for a (locally) linear model. We obtain a joint distribution of all logits according to  $\mathbf{y}^* \sim \mathcal{N}(\mathbf{c}, \Sigma^*)$  with  $\Sigma^*$ . As the classification margins of our ensemble can be described as a linear function of these logits, they also follow normal distribution, with the parameters derived above:

$$\bar{\mathbf{z}} \sim \mathcal{N}(\bar{\boldsymbol{\mu}}, \bar{\Sigma}) \quad (5)$$

As  $\bar{z}_i > 0$ ,  $\forall 2 \leq i \leq m$  corresponds to positive classification margins, and hence the prediction of majority class 1, we can integrate the corresponding probability density function over the positive quadrant in which  $\bar{\mathbf{z}} > 0$  holds to obtain the probability of an ensemble of  $k$  classifiers predicting the majority class 1:

$$p_1 = \mathcal{P}(\bar{F}(\mathbf{x} + \epsilon) = 1) = \mathcal{P}(\bar{z}_i > 0 : \forall 2 \leq i \leq m) = \int_{\substack{\bar{\mathbf{z}} \text{ s.t. } \bar{z}_i > 0, \\ \forall 2 \leq i \leq m}} \mathcal{P}_{\bar{\mathbf{Z}} \sim \mathcal{N}(\bar{\mu}, \bar{\Sigma})}(\bar{\mathbf{Z}} = \bar{\mathbf{z}}) d\mathbf{z}.$$

We evaluate this expression numerically, using Monte Carlo Integration with  $10^7$  samples. Based on the thus obtained success probability of an individual perturbed sample to be classified as majority class, we can calculate a probability distribution over the certifiable radii for a given smoothing parameter set consisting of confidence level  $\alpha$ , perturbation sample number  $n$  and perturbation variance  $\sigma_\epsilon^2$  as:

$$\mathcal{P}(R = \sigma_\epsilon \Phi^{-1}(\underline{p}_1(n_1, n, \alpha))) = \mathcal{B}(n_1, n, p_1)$$

with the probability  $\mathcal{B}(s, r, p)$  of drawing  $s$  successes in  $r$  trials from a Binomial distribution with success probability  $p$ , and the lower confidence bound  $\underline{p}(s, r, \alpha)$  to the success probability of a Bernoulli experiment given  $s$  successes in  $r$  trials with confidence  $\alpha$  according to the Clopper-Pearson interval [53].

## C Proof of Theorem 6.1

We first restate the theorem:

**Theorem** (Theorem 6.1 restated). *For  $\alpha, \beta \in [0, 1]$ ,  $s \in \mathbb{N}^+$ ,  $n_1 < \dots < n_s$ , CERTIFYADP:*

1. *returns  $\hat{c}_A$  if at least  $1 - \alpha$  confident that  $G$  is robust with radius at least  $r$ .*
2. *returns  $\emptyset$  before stage  $s$  only if at least  $1 - \beta$  confident that  $G$  is not robust at radius  $r$ .*
3. *for  $n_s \geq \lceil n(1 - \log_\alpha(s)) \rceil$  has maximum certifiable radii at least as large as CERTIFY for  $n$ .*

*Proof.* We show statements 1, 2, and 3 individually.

*Proof of 1.* If a phase in CERTIFYADP returns  $\hat{c}_A$ , then via theorem 3.1,  $G$  will be not robust with probability at most  $\alpha/s$ . Via Bonferroni correction [59], if CERTIFYADP returns  $\hat{c}_A$ , then  $G$  is robust with radius at least  $r$  with confidence  $1 - s(\alpha/s) = 1 - \alpha$ .

*Proof of 2.* If CERTIFYADP returns  $\emptyset$  in phase  $s$ , we have  $\overline{p}_A < p'_A = \Phi(r/\sigma_\epsilon)$  the minimum success probability for certification at  $r$ . By the definition of the UPPERCONFIDENCEBOUND the true success probability of  $G$  will be  $p_A \leq \overline{p}_A$  with confidence at least  $\beta/(s-1)$ . Hence, if phase  $j$  returns  $\emptyset$ ,  $G$  will be none-robust at radius  $r$  with confidence  $1 - \beta/(s-1)$ . Again with Bonferroni correction [59], the overall probability that  $G$  is robust at  $r$  despite CERTIFYADP abstaining early is at most  $(s-1)(\beta/(s-1)) = \beta$ .

*Proof of 3.* Finally, to prove the last part, we assume  $\text{cnts}[\hat{c}_A] = n$ , yielding the largest certifiable radii for any given  $n$  and  $\alpha$ . Now, the largest radius provable via Theorem 3.1 with  $n$  samples at  $\alpha$  is  $\alpha^{1/n}$  [5]. Similarly, for  $n_s$  samples at  $\alpha/s$ , it is  $(\frac{\alpha}{s})^{\frac{1}{n_s}}$ . Then we have the following equivalences:

$$(\alpha)^{\frac{1}{n}} = \left(\frac{\alpha}{s}\right)^{\frac{1}{n_s}} \Leftrightarrow \alpha^{n_s} = \left(\frac{\alpha}{s}\right)^n \Leftrightarrow n_s \log \alpha = n(\log \alpha - \log s) \Leftrightarrow n_s = n(1 - \log_\alpha(s))$$

Hence, if we choose  $n_s = \lceil n(1 - \log_\alpha(s)) \rceil$ , then we can certify at least the same maximum radius with  $n_s$  samples at  $\alpha/s$  as with  $n$  samples at  $\alpha$ . Thus, overall, we can certify the same maximum radius at  $\alpha$ .  $\square$

## D Experimental Details

In this section, we provide greater detail on the datasets, architectures, and training and evaluation methods used for our experiments.

### D.1 Dataset Details

We use the CIFAR10 and ImageNet datasets in our experiments.

CIFAR10 [56] (MIT License) contains 50'000 training and 10'000 test set images partitioned into 10 classes. We evaluate every  $20^{th}$  image of the test set starting with index 0 (0, 20, 40, ..., 9980) in our experiments.

ImageNet [57] contain 1'287'167 training and 50'000 validation images, partitioned into 1000 classes. We evaluate every  $100^{th}$  image of the validation set starting with index 0 (0, 100, 200, ..., 49900) in our experiments.

### D.2 Architecture Details

We use different versions of ResNet [10] for our experiments. Concretely, we evaluate ensembles of ResNet20 and ResNet110 on CIFAR10 and ensembles of ResNet50 on ImageNet.

ResNet110 has about 6.35 times as many parameters as ResNet20 (see Table 7). ResNet50 instantiated for ImageNet has substantially more parameters than ResNet110 instantiated for CIFAR10, because of the significantly larger input dimension of ImageNet samples.

Table 7: Parameter count of the used network architectures

Dataset	Architecture	Parameter count
CIFAR10	ResNet20	272'474
	ResNet110	1'730'714
ImageNet	ResNet50	25'557'032

### D.3 Training Methods

To obtain high certified radii via RS, the base model  $F$  must be trained to cope with the added Gaussian noise  $\epsilon$ . To this end, Cohen et al. [5] propose data augmentation with Gaussian noise during training, referred to as GAUSSIAN in the following. Building on this Salman et al. [6] suggest SMOOTHADV, a combination of adversarial training [13, 14, 60] with this data augmentation. (Here we always consider the PGD version.) While improving accuracy, this training procedure is computationally expensive. MACER [7], achieves similar performance with a cheaper training procedure, adding a loss term directly optimizing a surrogate certification radius. Jeong and Shin [8], called CONSISTENCY, in the following, replace this term by a more easily optimizable loss, further decreasing training time and improving performance. Depending on the setting, the current state-of-the-art results are either achieved by SMOOTHADV, MACER, CONSISTENCY or a combination thereof.

Further, Salman et al. [45] present denoised smoothing, where the base classifier  $f = h \circ f'$  is the composition of a denoiser  $h$  that removes the Gaussian noise from the input and an underlying classifier  $f'$  that is not specially adapted to Gaussian noise, e.g., accessed via an API.

### D.4 Training Details

All models are implemented in PyTorch [58] (customized BSD licence).

For GAUSSIAN training (No license specified), we use the published code by Cohen et al. [5]. For each network, we chose a different random seed otherwise using identical parameters. Overall, we trained 50 ResNet20 and 10 ResNet110 for each  $\sigma_\epsilon \in \{0.25, 0.5, 1.0\}$ . The ImageNet results, we have taken from their GitHub.

For CONSISTENCY training (MIT License), we use the code published by Jeong and Shin [8] and CONSISTENCY instantiation built on GAUSSIAN training. Similarly to GAUSSIAN, we use a different random seed and otherwise identical parameters. We chose the parameters reported to yield the largest ACR by Jeong and Shin [8] for any given  $\sigma_\epsilon$ . In detail, for CIFAR10 we generally use  $\eta = 0.5$ , using  $\lambda = 20$  for  $\sigma_\epsilon = 0.25$  and  $\lambda = 10$  for  $\sigma_\epsilon = 0.5$  and  $\sigma_\epsilon = 1.0$  (all for both ResNet20 and ResNet110). In this way, we train 50 ResNet20 and 10 ResNet110 for each  $\sigma_\epsilon \in \{0.25, 0.5, 1.0\}$ . For ImageNet, we use  $\eta = 0.1$  and  $\lambda = 5$  training only models at  $\sigma_\epsilon = 1.0$ .

Table 8: Reference training times for individual models on GeForce RTX2080 Tis

Dataset	Training	Architecture	#GPUs	time per Epoch [s]	total time [h]
CIFAR10	GAUSSIAN	ResNet110	1	41.8	1.74
		ResNet20	1	9.6	0.40
	CONSISTENCY	ResNet110	1	79.5	3.31
		ResNet20	1	18.5	0.77
	SMOOTHADV	ResNet110	1	660	27.5
ImageNet	CONSISTENCY	ResNet50	4	3420	85

For SMOOTHADV training (MIT License) we use the PGD based instantiation of the code published by Salman et al. [6]. Note that due to the long training times, we only train SMOOTHADV models ourselves for CIFAR10 at  $\sigma_\epsilon = 1.0$ , because in that case the performance discrepancies between the best and other published models were too large to construct effective ensembles. The individual models, we train, only differ by random seed, all using PGD attacks with  $T = 10$  steps, an  $\epsilon = 512/255$ , 10 epochs of warm-up, and  $m_{\text{train}} = 2$  noise terms per sample during training.

We use the same training schedule and optimizer for all models, i.e. stochastic gradient descent with Nesterov momentum (weight = 0.9, no dampening), with an  $\ell_2$  weight decay of 0.0001. For CIFAR10, we use a batch size of 256 and an initial learning rate of 0.1 reducing it by a factor of 10 every 50 epochs and training for a total of 150 epochs.

For ImageNet, we use the same settings, only reducing the total epoch number to 90, and decreasing the learning rate every 30 epochs.

All single MACER (No license specified) and SMOOTHADV (MIT License) (except CIFAR10 at  $\sigma_\epsilon = 1.0$ ) trained models are taken directly from Zhai et al. [7] and Salman et al. [6], respectively.

For our experiments on denoised smoothing, we use the 4 white box denoisers with DNCNN-WIDE architecture trained with learning schedules 1, 3, 4, and 5 for STAB ResNet110, and the ResNet110 trained on unperturbed samples for 90 epochs from Salman et al. [45] (MIT License).

To rank the single models for CIFAR10, we have evaluated them on a disjunct hold-out portion of the CIFAR10 test set. Concretely, we use the test images with indices 1, 21, 41, ..., 9981 to rank the single models for both GAUSSIAN and CONSISTENCY trained models. The performance of individual models values we report are those of the models with the best score on this validation set for CIFAR10 and the best score on the test set for ImageNet (favouring individual models in this setting). For ensembles of size  $k < 10$  and  $k < 50$  for ResNet110 and ResNet20 respectively, we ensemble the  $k$  models according to their performance on the holdout set. We note, that other combinations might yield stronger ensembles, but an exhaustive search of all combinatorially many possibilities is computationally infeasible.

CIFAR10 models were trained on single GeForce RTX 2080 Ti and ImageNet models on quadruple 2080 Tis. We report the epoch-wise and total training times for individual models in Table 8 (when trained sequentially one at a time).

## D.5 Experiment Timings

To evaluate the ensembles of ResNet20 and ResNet110 on CIFAR10, we use single GeForce RTX 2080 Ti and to evaluate ensembles of ResNet50 on ImageNet we use double 2080 Tis.

For both datasets, 500 samples are evaluated per experiment as discussed in App. D.1. Below we list the time required for certification using CERTIFY and no  $K$ -Consensus aggregation:

- ResNet110 on CIFAR10 (1 GPU): 4.12h per single model; 41.2h per ensemble of 10
- ResNet20 on CIFAR10 (1 GPU): 0.825h per single model; 41.3h per ensemble of 50
- ResNet50 on ImageNet (2 GPUs): 8.75h per single model; 26.2h per ensemble of 3

The timing for different ensemble sizes scales linearly between full size and individual model timings. The time required for certification using CERTIFYADP and/or  $K$ -Consensus aggregation can be obtained by dividing the timings reported above with the speed-up factor TimeRF reported for the corresponding experiments.

Table 9: Average certified radius (ACR) and certified accuracy at various radii for ensembles of  $k$  models ( $k = 1$  are single models) on CIFAR10. Larger is better.

$\sigma_\epsilon$	Training	Architecture	$k$	ACR	Radius r										
					0.0	0.25	0.50	0.75	1.00	1.25	1.50	1.75	2.00	2.25	2.50
0.25	GAUSSIAN	ResNet110	1	0.450	77.6	60.0	45.6	30.6	0.0	0.0	0.0	0.0	0.0	0.0	0.0
			10	<b>0.541</b>	<b>83.4</b>	<b>70.6</b>	55.4	42.0	0.0	0.0	0.0	0.0	0.0	0.0	
		ResNet20	1	0.434	77.4	63.4	43.6	26.6	0.0	0.0	0.0	0.0	0.0	0.0	
			5	0.500	80.2	65.4	50.4	36.8	0.0	0.0	0.0	0.0	0.0	0.0	
	CONSISTENCY	ResNet110	1	0.546	75.6	65.8	57.2	46.4	0.0	0.0	0.0	0.0	0.0	0.0	
			10	<b>0.583</b>	76.8	70.4	<b>60.4</b>	<b>51.6</b>	0.0	0.0	0.0	0.0	0.0	0.0	
		ResNet20	1	0.528	71.8	64.2	55.6	45.2	0.0	0.0	0.0	0.0	0.0	0.0	
			5	0.547	73.0	65.4	57.6	47.6	0.0	0.0	0.0	0.0	0.0	0.0	
	MACER	ResNet110	1	0.551	73.0	64.8	57.0	50.2	0.0	0.0	0.0	0.0	0.0	0.0	
			50	0.518	77.4	69.0	52.6	39.4	0.0	0.0	0.0	0.0	0.0	0.0	
SMOOTHADV	ResNet110	1	0.546	73.6	66.8	57.2	46.8	0.0	0.0	0.0	0.0	0.0	0.0	0.0	
0.50	GAUSSIAN	ResNet110	1	0.535	65.8	54.2	42.2	32.4	22.0	14.8	10.8	6.6	0.0	0.0	0.0
			10	0.648	<b>69.0</b>	<b>60.4</b>	<b>49.8</b>	40.0	29.8	19.8	15.0	9.6	0.0	0.0	0.0
		ResNet20	1	0.534	65.2	55.0	43.0	33.0	22.4	16.2	9.6	5.0	0.0	0.0	0.0
			5	0.615	67.6	58.4	47.4	38.8	27.4	19.8	13.2	7.0	0.0	0.0	0.0
	CONSISTENCY	ResNet110	1	0.630	67.2	59.4	48.6	39.2	29.0	21.6	14.6	8.2	0.0	0.0	0.0
			10	0.708	63.2	54.8	48.8	42.0	36.0	29.8	22.4	16.4	0.0	0.0	0.0
		ResNet20	1	<b>0.756</b>	65.0	59.0	49.4	<b>44.8</b>	38.6	32.0	26.2	19.8	0.0	0.0	0.0
			5	0.691	62.6	55.2	47.4	41.8	34.6	28.4	21.8	16.8	0.0	0.0	0.0
	MACER	ResNet110	1	0.723	62.2	55.0	48.6	42.6	36.4	29.8	23.4	20.6	0.0	0.0	0.0
			50	0.729	61.6	55.8	49.2	43.0	37.8	30.6	24.2	20.0	0.0	0.0	0.0
	SMOOTHADV	ResNet110	1	0.668	62.4	54.4	48.2	40.2	33.2	26.8	19.8	13.0	0.0	0.0	0.0
			1	0.725	57.4	50.6	45.8	42.4	37.6	32.2	27.8	22.0	0.0	0.0	0.0
		ResNet110	1	0.697	50.2	46.2	44.4	39.6	37.6	32.6	28.6	23.4	0.0	0.0	0.0
			1	0.710	52.4	47.6	45.0	40.6	37.6	33.4	28.2	23.4	0.0	0.0	0.0
1.00	GAUSSIAN	ResNet110	1	0.532	48.0	40.0	34.4	26.6	22.0	17.2	13.8	11.0	9.0	5.8	4.2
			10	0.607	49.4	<b>44.0</b>	37.6	29.6	24.8	20.0	16.4	13.6	11.2	9.4	6.8
		ResNet20	1	0.538	48.0	41.2	35.0	27.8	21.6	17.8	14.8	12.0	9.0	5.6	3.4
			5	0.590	49.2	42.8	37.8	30.4	24.0	19.4	16.2	13.8	11.2	8.2	5.0
	CONSISTENCY	ResNet110	1	0.597	<b>49.6</b>	43.0	37.4	30.4	23.6	18.6	15.8	13.6	11.2	9.0	5.0
			10	0.778	45.4	41.6	37.4	33.6	28.0	25.6	23.4	19.6	17.4	16.2	14.6
		ResNet20	1	0.809	46.4	42.6	37.2	33.0	29.4	25.6	23.2	21.0	17.6	16.2	14.6
			5	0.757	43.6	39.8	34.8	30.8	27.6	24.6	22.6	19.4	17.4	15.4	13.8
	MACER	ResNet110	5	0.779	43.4	40.0	35.6	32.2	28.0	24.8	22.2	20.4	17.4	15.8	13.8
			50	0.788	45.2	40.6	36.4	32.4	28.2	24.6	22.0	20.2	17.8	16.0	14.6
	SMOOTHADV	ResNet110	1	0.797	42.8	40.6	37.4	34.4	31.0	28.0	25.0	21.4	18.4	15.0	13.8
			1	0.844	45.4	41.0	38.0	34.8	32.2	28.4	25.0	<b>22.4</b>	19.4	<b>16.6</b>	<b>14.8</b>
		ResNet110	10	<b>0.855</b>	44.8	40.6	<b>38.2</b>	<b>35.6</b>	<b>32.6</b>	<b>29.2</b>	<b>25.8</b>	22.0	<b>19.8</b>	15.8	<b>14.8</b>

## E Additional Experiments

In the following, we present numerous additional experiments and more detailed results for some of the experiments presented in section 7.

### E.1 Additional Results on CIFAR10

In this section, we present more experimental results on CIFAR10. Concretely, Table 9 presents the performance of ensembles of ResNet20 ( $k \in \{1, 5, 50\}$ ) and ResNet110 ( $k \in \{1, 10\}$ ) trained using a range of methods for  $\sigma_\epsilon = 0.25$ ,  $\sigma_\epsilon = 0.5$ , and  $\sigma_\epsilon = 1.0$ . We again consistently observe that ensembles significantly outperform their constituting models, leading to a new state-of-the-art both in ACR and at most radii at  $\sigma_\epsilon = 0.25$ ,  $\sigma_\epsilon = 0.5$ , and  $\sigma_\epsilon = 1.0$ .

### E.2 Additional Results on ImageNet

In Table 10 we provide more detailed results on ImageNet for ensembles of ResNet50 at  $\sigma_\epsilon = 1.0$ . In particular, we include the performance of all individual classifiers which constitute the ensembles, where  $k = 3$  combines all three and  $k = 2$  the first two for CONSISTENCY and the last two for SMOOTHADV. Note that the SMOOTHADV models are taken directly from Salman et al. [6] and

Table 10: Average certified radius (ACR) and the certified accuracy at various radii on ImageNet for ensembles of  $k$  ResNet50 ( $k = 1$  are single models) at  $\sigma_\epsilon = 1.0$ . Larger is better.

Training	$k$	ACR	Radius r							
			0.0	0.50	1.00	1.50	2.00	2.50	3.00	3.50
CONSISTENCY	1	1.022	43.2	39.8	35.0	29.4	24.4	22.2	16.6	13.4
	1	0.990	42.0	37.2	34.4	29.6	24.8	20.2	16.0	13.4
	1	1.006	41.6	38.6	35.2	29.6	25.4	21.2	17.6	13.8
	2	1.086	<b>44.8</b>	<b>41.0</b>	36.6	32.4	27.4	22.4	19.4	15.6
	3	<b>1.108</b>	44.6	40.2	<b>37.2</b>	<b>34.0</b>	<b>28.6</b>	23.2	20.2	16.4
SMOOTHADV	1	1.011	40.6	38.6	33.8	29.8	25.6	20.6	18.0	14.4
	1	1.002	39.4	35.4	32.0	29.2	25.6	22.2	20.0	16.4
	1	0.927	32.0	30.8	28.6	26.0	23.6	21.0	19.2	18.6
	2	1.022	37.4	33.4	31.4	29.4	26.6	23.8	21.0	18.6
	3	1.065	38.6	36.0	34.0	30.0	27.6	<b>24.6</b>	<b>21.2</b>	<b>18.8</b>
GAUSSIAN	1	0.875	43.6	37.8	32.6	26.0	19.4	14.8	12.2	9.0

were trained with a different  $\epsilon$  parameter (256, 512, and 1024). We observe that if there is a large discrepancy between model performance at some radii (e.g., the SMOOTHADV models at small radii), then the ensemble might perform worse than the strongest constituting model. Overall and when performance is homogenous, however, ensembles once again obtain significant performance increases over individual models, yielding state-of-the-art ACR and accuracy at every radius.

### E.3 Additional Ensemble Experiments

In this section, we present a range of experiments on different aggregation approaches, the effect of ensemble size, and the variability of our results.

#### E.3.1 Aggregation Approaches

We experiment with various instantiations of the general aggregation approach described in §4. In particular, we consider soft-voting, hard-voting, soft-voting after softmax, and weighted soft-voting.

**Soft-voting** We simply average the logits to obtain

$$\bar{f}(\mathbf{x}) = \frac{1}{k} \sum_{l=1}^k f^l(\mathbf{x}).$$

**Hard-voting** We process the outputs of single models with the post-processing function  $\gamma_{HV}(\mathbf{y}^l) = \mathbf{1}_{j=\arg \max_i(y_i^l)}$  that provides a one-hot encoding of the  $\arg \max$  of  $f^l(\mathbf{x})$ , before averaging to obtain

$$\bar{f}(\mathbf{x}) = \frac{1}{k} \sum_{l=1}^k \mathbf{1}_{j=\arg \max_i(f^l(\mathbf{x})_i)}.$$

**Soft-voting after softmax** We process the outputs of the single models, by applying the softmax function as post-processing function  $\gamma_{softmax}$  to obtain

$$\bar{f}(\mathbf{x}) = \frac{1}{k} \sum_{l=1}^k \frac{\exp(f^l(\mathbf{x}))}{\sum_i \exp(f^l(\mathbf{x})_i)}.$$

**Weighted soft-voting** We consider soft-voting with a classifier-wise weights  $w^l$  learned on a separate holdout set and obtain

$$\bar{f}(\mathbf{x}) = \frac{1}{k} \sum_{l=1}^k w^l f^l(\mathbf{x}).$$

We compare these approaches in Table 11 and observe that the two soft-voting schemes perform very similarly and outperform the other approaches. We decide to use soft-voting without soft-max for its conceptual simplicity for all other experiments.

Table 11: Comparison of various aggregation methods for ensembles of 10 ResNet110 at  $\sigma_\epsilon = 0.25$  on CIFAR10. Larger is better.

Training	Aggregation method	ACR	Radius r			
			0.00	0.25	0.50	0.75
GAUSSIAN	soft-voting	<b>0.541</b>	83.4	70.6	<b>55.4</b>	<b>42.0</b>
	hard-voting	0.529	83.8	69.4	53.2	40.6
	soft-voting after softmax	0.540	<b>84.0</b>	<b>70.8</b>	55.2	41.8
	weighted soft-voting	0.538	83.4	70.4	54.6	41.8
CONSISTENCY	soft-voting	0.583	76.8	70.4	60.4	51.6
	hard-voting	0.574	<b>77.2</b>	69.6	60.0	50.6
	soft-voting after softmax	<b>0.584</b>	77.0	70.4	<b>60.6</b>	<b>51.8</b>
	weighted soft-voting	0.579	76.4	<b>70.6</b>	59.6	51.2

Table 12: Effect of ensemble size  $k$  on ACR and certified accuracy at different radii, for GAUSSIAN and CONSISTENCY trained ResNet20. Larger is better.

Training	$\sigma_\epsilon$	$k$	ACR	Radius r										
				0.0	0.25	0.50	0.75	1.00	1.25	1.50	1.75	2.00	2.25	2.50
GAUSSIAN	0.25	1	0.434	77.4	63.4	43.6	26.6	0.0	0.0	0.0	0.0	0.0	0.0	0.0
		3	0.486	79.6	66.0	49.6	34.6	0.0	0.0	0.0	0.0	0.0	0.0	0.0
		5	0.500	80.2	65.4	50.4	36.8	0.0	0.0	0.0	0.0	0.0	0.0	0.0
		10	0.510	<b>80.4</b>	67.4	51.8	37.4	0.0	0.0	0.0	0.0	0.0	0.0	0.0
		50	<b>0.517</b>	<b>80.4</b>	<b>68.6</b>	<b>52.8</b>	<b>38.8</b>	0.0	0.0	0.0	0.0	0.0	0.0	0.0
	1.0	1	0.538	48.0	41.2	35.0	27.8	21.6	17.8	14.8	12.0	9.0	5.6	3.4
		3	0.579	49.2	42.8	36.4	30.2	23.0	18.8	15.6	13.0	10.8	7.4	4.4
		5	0.590	49.2	42.8	<b>37.8</b>	<b>30.4</b>	<b>24.0</b>	<b>19.4</b>	<b>16.2</b>	<b>13.8</b>	<b>11.2</b>	8.2	<b>5.0</b>
		10	0.592	48.8	42.8	37.0	<b>30.4</b>	23.6	19.0	16.2	13.6	11.0	<b>9.2</b>	<b>5.0</b>
		50	<b>0.597</b>	<b>49.6</b>	<b>43.0</b>	37.4	<b>30.4</b>	23.6	18.6	15.8	13.6	<b>11.2</b>	9.0	<b>5.0</b>
CONSISTENCY	0.25	1	0.528	71.8	64.2	55.6	45.2	0.0	0.0	0.0	0.0	0.0	0.0	0.0
		3	0.544	<b>73.2</b>	65.2	<b>57.6</b>	47.6	0.0	0.0	0.0	0.0	0.0	0.0	0.0
		5	0.547	73.0	<b>65.4</b>	<b>57.6</b>	47.6	0.0	0.0	0.0	0.0	0.0	0.0	0.0
		10	0.547	72.2	65.0	57.4	48.8	0.0	0.0	0.0	0.0	0.0	0.0	0.0
		50	<b>0.551</b>	73.0	64.8	57.0	<b>50.2</b>	0.0	0.0	0.0	0.0	0.0	0.0	0.0
	1.0	1	0.757	43.6	39.8	34.8	30.8	27.6	24.6	<b>22.6</b>	19.4	17.4	15.4	13.8
		3	0.777	44.2	39.6	<b>36.8</b>	31.8	28.4	<b>25.0</b>	22.4	19.8	17.6	15.6	14.0
		5	0.779	43.4	40.0	35.6	32.2	28.0	24.8	22.2	<b>20.4</b>	17.4	15.8	13.8
		10	0.784	44.4	<b>40.6</b>	36.4	32.2	<b>29.2</b>	24.2	22.2	<b>20.4</b>	17.6	<b>16.0</b>	14.2
		50	<b>0.788</b>	<b>45.2</b>	<b>40.6</b>	36.4	<b>32.4</b>	28.2	24.6	22.0	20.2	<b>17.8</b>	<b>16.0</b>	<b>14.6</b>

### E.3.2 Ensemble Size

In Table 12, we present extended results on the effect of ensemble size for different training methods, and  $\sigma_\epsilon$ . Generally, we observe that ensembles of size 3 and 5 already significantly improve over the performance of a single model, while further increasing the ensemble size mostly leads to marginal gains. This aligns well with our theory from §5.

### E.3.3 Variability of Results

In table 13, we report mean and standard deviation of ACR and certified accuracy for 50 GAUSSIAN and CONSISTENCY trained ResNet20 with different random seeds, either combined to 10 ensembles with  $k = 5$  or evaluated individually. Generally, we observe a notably smaller standard deviation of the ensembles compared to individual models. We visualize this in Fig. 7, where we show the  $\pm 3\sigma$  region.

### E.4 Additional K-Consensus Experiments

In Table 14 we present a more detailed version of Table 2. We emphasize that for  $K = 5$  and  $K = 10$  for ResNet110 and ResNet20, respectively, we achieve the same ACR as with the full ensemble, while reducing the certification time by a factor of 1.59 and 2.01, respectively.

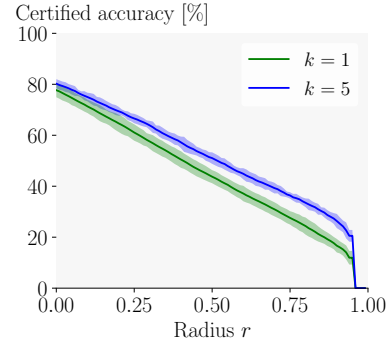


Figure 7: Mean and  $\pm 3\sigma$  interval of certified accuracy over radius  $r$  computed over 50 GAUSSIAN trained ResNet20.

Table 13: Mean and standard deviation of ACR and certified accuracy for CIFAR10 at various radii for 50 ResNet20 with different random seeds either evaluated as 10 ensembles with  $k = 5$  or as individual models at  $\sigma_\epsilon = 0.25$ .

Training	$k$	ACR	Radius $r$		
			0.25	0.50	0.75
GAUSSIAN	1	$0.4350 \pm 0.0046$	$61.08 \pm 1.08$	$43.74 \pm 0.86$	$27.58 \pm 0.88$
	5	$0.4994 \pm 0.0025$	$66.58 \pm 0.62$	$51.04 \pm 0.76$	$36.38 \pm 0.42$
CONSISTENCY	1	$0.5202 \pm 0.0049$	$63.57 \pm 0.86$	$54.22 \pm 1.03$	$44.30 \pm 0.89$
	5	$0.5445 \pm 0.0017$	$64.90 \pm 0.66$	$56.86 \pm 0.49$	$47.94 \pm 0.68$

Table 14: Effect of  $K$ -Consensus aggregation on CONSISTENCY trained ensembles of 10 ResNet110 and 50 ResNet20 on CIFAR10 at  $\sigma_\epsilon = 0.25$ .

Architecture	$K$	ACR	Radius $r$				TimeRF	KCR [%]
			0.0	0.25	0.50	0.75		
ResNet110	2	0.576	77.2	70.2	60.0	50.4	3.25	85.8
	3	0.581	77.0	70.0	60.6	51.6	2.29	79.7
	5	0.583	76.8	70.4	60.4	51.6	1.59	74.2
	10	0.583	76.8	70.4	60.4	51.6	1.00	0.0
ResNet20	2	0.544	72.2	65.2	57.0	48.4	6.50	87.7
	3	0.549	72.6	65.0	57.4	50.0	4.41	82.4
	5	0.550	72.8	65.0	57.0	50.2	2.99	76.4
	10	0.551	73.0	64.8	57.0	50.2	2.01	69.8
	50	0.551	73.0	64.8	57.0	50.2	1.00	0.0

## E.5 Additional Adaptive Sampling Experiments

**Adaptive sampling for ensembles on CIFAR10** For comparison with Table 5, where we show the combined effect of  $K$ -Consensus aggregation and adaptive sampling, we show the results for just applying adaptive sampling to the same setting in Table 15, using  $\{n_j\} = \{1'000, 10'000, 125'000\}$ ,  $\sigma_\epsilon = 0.25$ , and ensembles of 10 CONSISTENCY trained ResNet110. We observe that the speed-ups for small radii are comparable to applying both  $K$ -Consensus aggregation and adaptive sampling, as only few samples have to be evaluated. The additional benefit due to  $K$ -Consensus aggregation grows, as the later certification stages are entered more often for larger radii, highlighting the complementary nature of the two methods. Note that for radius  $r = 0.75$ , 1'000 samples are never sufficient for certification, but can still yield early abstentions.

**Adaptive sampling and  $K$ -consensus** In Table 16, we show the effect of adaptive sampling and  $K$ -Consensus aggregation for GAUSSIAN trained ResNet110 on CIFAR10, analogously to Table 5 (for CONSISTENCY trained models). We confirm our previous observation that the sample reduction is most prominent for small radii (for a given  $\sigma_\epsilon$ ) while KCR increases with radius.

**Adaptive sampling for ImageNet ensembles** In Table 17, we demonstrate the applicability of our adaptive sampling approach to ensembles of ResNet50 on ImageNet. In particular, we achieve sampling reduction factors of up to 30 without incurring an accuracy penalty. For a fixed  $\sigma_\epsilon$ , we empirically observe larger speed-ups at smaller radii. This effect however depends on the underlying distribution of success probabilities and would be expected to invert for a model that has true success probabilities close to  $p_A \approx 0.5$  for most samples.

**Effect of sampling stage sizes** Additionally, in table 18, we investigate how the choice of the number of phases, and the number of samples in each phase influence the sampling gain for various radii and models. We observe that as few as 100 samples can be sufficient to certify or abstain from up to 80% of samples, making schedules with many phases attractive. However, when the true success probability is close to the one required for certification a large number of samples is required to obtain sufficiently tight confidence bounds on the success probability to decide either way. This leads to many samples being discarded for schedules with many phases. Additionally, the higher per



Table 15: Effect of adaptive sampling with  $\{n_j\} = \{1'000, 10'000, 125'000\}$  for ensembles of 10 CONSISTENCY trained ResNet110 on ImageNet at  $\sigma_\epsilon = 0.25$ .  $ASA_j$  and  $ASC_j$  are the percentages of samples abstained from and certified in phase  $j$ , respectively

Radius	acc <sub>cert</sub> [%]	ASA <sub>1</sub>	ASC <sub>1</sub>	ASA <sub>2</sub>	ASC <sub>2</sub>	ASA <sub>3</sub>	ASC <sub>3</sub>	SampleRF	TimeRF
0.25	70.4	15.2	80.6	0.6	3.0	0.6	0.0	<b>46.17</b>	<b>43.29</b>
0.50	60.4	26.0	64.8	4.2	2.0	2.0	1.0	18.61	17.27
0.75	52.0	36.4	0.0	3.6	51.4	3.4	5.2	5.99	5.49

Table 16: Adaptive sampling with  $\{n_j\} = \{1'000, 10'000, 125'000\}$  and  $K$ -consensus early stopping with  $K = 6$  on CIFAR10 with an ensemble of 10 GAUSSIAN trained ResNet110. Sample and time gain are the reduction factor in comparison to standard sampling with  $n = 100'000$  (larger is better).  $ASR_j$  is the percentage of samples returned in phase  $j$ . KCR is the percentage of samples for which only  $K$  classifiers were evaluated.

Radius	$\sigma_\epsilon$	acc <sub>cert</sub> [%]	ASR <sub>1</sub>	ASR <sub>2</sub>	ASR <sub>3</sub>	SampleRF	KCR	TimeRF
0.25	0.25	70.6	93.4	5.2	1.4	<b>30.30</b>	35.6	31.2
0.50	0.25	55.6	90.2	6.8	3.0	18.43	57.3	21.1
0.75	0.25	41.8	49.6	42.2	8.2	6.64	86.8	8.9
1.00	0.50	30.2	84.8	11.4	3.8	14.64	74.6	18.2
1.25	1.00	20.2	91.0	6.2	2.8	19.51	65.3	23.3
1.50	1.00	16.6	92.6	6.0	1.4	29.65	69.8	<b>36.4</b>
1.75	1.00	13.8	94.0	4.2	1.8	26.98	76.4	34.5
2.00	1.00	11.4	93.8	4.4	1.8	26.85	79.6	34.9
2.25	1.00	9.4	90.4	7.6	2.0	23.48	84.5	11.5
2.50	1.00	6.4	88.4	7.4	4.2	14.35	<b>89.9</b>	20.4

phase confidence required due to Bonferroni correction requires more samples to be drawn to be able to obtain the same maximum lower confidence bound to the success probability. This latter effect becomes especially pronounced for larger radii, where higher success probabilities are required.

Table 17: Adaptive sampling with  $\{n_j\} = \{1'500, 15'000, 125'000\}$  for  $r \leq 3.0$  and  $\{n_j\} = \{3'000, 30'000, 125'000\}$   $r = 3.5$  on ImageNet with an ensemble of 3 CONSISTENCY trained ResNet50. SampleRF and TimeRF are the reduction factor in comparison certification with CERTIFY with  $n = 100'000$ .  $ASR_j$  is the percentage of samples returned in phase  $j$ .

Radius	acc <sub>cert</sub> [%]	ASR <sub>1</sub>	ASR <sub>2</sub>	ASR <sub>3</sub>	SampleRF	TimeRF
0.50	40.2	93.8	4.4	1.8	22.66	20.7
1.00	37.2	95.0	4.0	1.0	<b>29.66</b>	<b>27.5</b>
1.50	34.0	93.0	5.6	1.4	24.50	22.4
2.00	28.6	89.8	8.6	1.6	21.13	19.3
2.50	23.0	86.4	10.6	3.0	14.86	13.4
3.00	19.8	70.0	25.6	4.4	9.54	8.6
3.50	16.4	74.8	3.4	21.8	3.27	2.6

Table 18: Effect of adaptive sampling for individual ResNet110 on CIFAR10 at  $\sigma_\epsilon = 0.25$ . ASA <sub>$j$</sub>  and ASC <sub>$j$</sub>  are the percentages of samples abstained from and certified in phase  $j$ , respectively. We compare multiple sampling count progressions  $\{n_j\}$ . More concretely, schedule 2<sub>1</sub> considers  $\{1'000, 115'000\}$ , 2<sub>2</sub> considers  $\{10'000, 115'000\}$ , 3<sub>1</sub> considers  $\{1'000, 10'000, 125'000\}$ , 3<sub>2</sub> considers  $\{2000, 15000, 125'000\}$ , 5<sub>1</sub> considers  $\{1'000, 4'000, 16'000, 64'000, 130'000\}$  and 5<sub>2</sub> considers  $\{100, 1'000, 5'000, 25'000, 130'000\}$ .

$\sigma_\epsilon$	Training	Schedule	acc <sub>cert</sub> [%]	ASA <sub>1</sub>	ASC <sub>1</sub>	ASA <sub>2</sub>	ASC <sub>2</sub>	ASA <sub>3</sub>	ASC <sub>3</sub>	ASA <sub>4</sub>	ASC <sub>4</sub>	ASA <sub>5</sub>	ASC <sub>5</sub>	SampleRF	TimeRF
0.25	GAUSSIAN	2 <sub>1</sub>	60.0	30.4	62.2	4.4	3.0	-	-	-	-	-	-	10.50	10.72
		2 <sub>2</sub>	60.2	33.8	63.8	0.8	1.6	-	-	-	-	-	-	7.93	8.04
		3 <sub>1</sub>	60.2	29.6	61.0	3.4	2.6	1.6	1.8	-	-	-	-	17.09	16.37
		3 <sub>2</sub>	60.0	31.6	62.0	2.0	2.0	1.2	1.2	-	-	-	-	17.96	16.92
		5 <sub>1</sub>	60.2	29.2	61.2	2.8	1.6	1.6	1.2	0.8	1.0	0.2	0.4	<b>28.12</b>	<b>20.65</b>
		5 <sub>2</sub>	60.0	19.8	53.2	10.6	7.8	2.0	2.0	1.2	0.8	1.4	1.2	22.56	17.25
	CONSISTENCY	2 <sub>1</sub>	66.0	20.6	75.4	2.8	1.2	-	-	-	-	-	-	17.69	17.60
		2 <sub>2</sub>	66.0	22.2	76.2	1.2	0.4	-	-	-	-	-	-	8.50	8.44
		3 <sub>1</sub>	66.0	20.4	75.4	2.0	0.6	1.0	0.6	-	-	-	-	30.17	28.30
		3 <sub>2</sub>	66.0	21.4	75.4	1.0	0.8	1.0	0.4	-	-	-	-	24.68	23.00
		5 <sub>1</sub>	66.0	20.2	74.8	1.4	0.6	0.6	0.8	0.8	0.2	0.4	0.2	36.09	26.89
		5 <sub>2</sub>	66.0	12.8	68.4	8.0	6.2	1.2	1.2	0.6	0.4	0.8	0.4	<b>44.43</b>	<b>33.73</b>
	GAUSSIAN	2 <sub>1</sub>	30.4	59.8	0.0	9.6	30.6	-	-	-	-	-	-	2.13	2.18
		2 <sub>2</sub>	30.4	65.0	24.6	4.4	6.0	-	-	-	-	-	-	4.76	4.70
		3 <sub>1</sub>	30.6	61.2	0.0	3.8	24.8	4.2	6.0	-	-	-	-	6.13	5.82
		3 <sub>2</sub>	30.6	61.2	0.0	4.2	27.6	3.8	3.2	-	-	-	-	6.74	<b>6.19</b>
		5 <sub>1</sub>	30.6	59.6	0.0	4.0	0.0	2.8	26.8	1.2	3.4	1.6	0.6	<b>8.78</b>	6.15
		5 <sub>2</sub>	30.6	48.2	0.0	11.4	0.0	3.8	0.0	3.2	29.0	2.6	1.8	7.04	5.45
0.75	CONSISTENCY	2 <sub>1</sub>	46.4	41.2	0.0	9.6	49.2	-	-	-	-	-	-	1.47	1.47
		2 <sub>2</sub>	46.4	46.6	43.6	4.2	5.6	-	-	-	-	-	-	4.91	4.72
		3 <sub>1</sub>	46.2	40.6	0.0	5.8	44.0	4.6	5.0	-	-	-	-	5.72	<b>5.27</b>
		3 <sub>2</sub>	46.6	43.2	0.0	4.4	45.0	3.0	4.4	-	-	-	-	5.68	5.08
		5 <sub>1</sub>	46.6	40.6	0.0	4.0	0.0	3.0	45.0	1.2	4.2	1.8	0.2	<b>6.95</b>	4.97
		5 <sub>2</sub>	46.2	32.6	0.0	8.6	0.0	4.2	0.0	2.4	46.4	3.2	2.6	4.96	3.88
	GAUSSIAN	2 <sub>1</sub>	30.4	59.8	0.0	9.6	30.6	-	-	-	-	-	-	2.13	2.18
		2 <sub>2</sub>	30.4	65.0	24.6	4.4	6.0	-	-	-	-	-	-	4.76	4.70
		3 <sub>1</sub>	30.6	61.2	0.0	3.8	24.8	4.2	6.0	-	-	-	-	6.13	5.82
		3 <sub>2</sub>	30.6	61.2	0.0	4.2	27.6	3.8	3.2	-	-	-	-	6.74	<b>6.19</b>